Physics – Uspekhi **63** (11) 1051 – 1071 (2020)

REVIEWS OF TOPICAL PROBLEMS

PACS numbers: 03.75.Hh, 03.75.Kk, **71.35.–y**, 71.35.Lk, **71.36.+c**, 72.15.Rn

Collective states of excitons in semiconductors

M M Glazov, R A Suris

DOI: https://doi.org/10.3367/UFNe.2019.10.038663

Contents

Abstract. **A review of many-body effects in exciton ensembles in semiconductors is given with the emphasis on two-dimensional systems: structures with single and double quantum wells and with quantum microcavities. The Bose–Einstein condensation effect, an accumulation of a macroscopic number of excitons in the ground state of the system, is discussed. The known prohibition on condensation in low-dimensional systems can be lifted due to the disorder resulting from the chaotic potential. Manifestations of the finite exciton lifetime and, correspondingly, of the nonequilibrium of the excitonic system caused by processes of excitons entering and leaving the condensate state are analyzed. Other collective phases of excitons, namely, two-dimensional crystals of dipolar excitons and an electron–hole liquid, formed as a result of interparticle interactions, are discussed.**

Keywords: exciton, Bose–Einstein condensate, superfluidity, disorder, dipolar exciton, exciton polariton

1. Introduction

Among the wide range of phenomena covered by condensed-matter physics, collective and many-body effects occupy an important place. A special role is played by effects where the quantum properties of particles are essentially manifested. Bose–Einstein condensation is the most striking among them. This effect, predicted in the 1920s, consists of the following. In a gas of noninteracting identical particles with integer spin (bosons) at a sufficiently low temperature, a certain fraction of particles occupies the ground state, i.e., condenses [1–3]. In a Bose gas, a phase transition occurs and an order parameter arises — the condensate wave function [4]. Physically, condensation occurs under the condition that the characteristic distance between particles is of the order of or less than their de Broglie wavelength. A simple estimate of the order of magnitude in a three-dimensional gas shows that condensation is possible at temperatures

$$T < T_{\mathrm{c}} \sim \frac{\hbar^2 N^{2/3}}{m k_{\mathrm{B}}}\,. \tag{1}$$

Here, N is the concentration of bosons and m is the boson mass. Below, we set the Planck constant $\hbar$ and the Boltzmann constant k_{B} equal to unity.

An interesting feature of Bose condensation is that the effect is possible in a noninteracting gas, in contrast to other phase transitions of both the first and second kind [3], where the interaction in the system is a driving force of the phase transition. Another exception is the transitions of the $2\frac{1}{2}$ kind, associated with a change in the topology of the Fermi surface [5, 6]. Convincing observations of Bose–Einstein condensation and pioneering studies of the condensate properties were carried out in the 1990s in atomic vapors of rubidium [7] (see also [8]) at ultralow temperatures of $\sim$ 170 nK. It is important to note that the repulsion between bosons does not destroy the condensate, but gives rise to a linear spectrum of elementary excitations in a Bose system with weak interaction [9]. Due to this fact, the condensate becomes superfluid.

Bose–Einstein condensation is possible not only in atomic systems but also in crystals for quasiparticles that obey Bose statistics. Excitons — electron–hole pairs in semiconductors and insulators, bound by Coulomb interaction — are in many respects analogs of atoms; thus, for example, the spectrum of the relative electron–hole motion in the Wannier–Mott exciton turns out to be hydrogen-like, and the exciton as a

---

M M Glazov, R A Suris Ioffe Institute,
ul. Politekhnicheskaya 26, 194021 St. Petersburg, Russian Federation
E-mail: glazov@coherent.ioffe.ru, suris@theory.ioffe.ru

Received 14 August 2019
Uspekhi Fizicheskikh Nauk **190** (11) 1121 – 1142 (2020)
Translated by V L Derbov

composite quasiparticle has an integer spin [10, 11]. In the 1960s, Moskalenko [12], Blatt, Böer and Brandt [13], Keldysh and Kozlov [14], and Gergel, Kazarinov, and Suris [15] drew attention to the possibility of condensation of large-radius excitons in semiconductors, and Agranovich and Toshich investigated the collective properties of Frenkel excitons, i.e., excitons of small radius comparable to the lattice parameter [16]. Since, at a given temperature, the wavelength of a particle is greater, the smaller the particle mass, excitons should condense at significantly higher temperatures than atoms (see Eqn (1)), and the possibility of generating and detecting excitons in relatively simple optical experiments opens up wide prospects for the study of exciton condensates.

Despite a number of studies carried out in the 1980s–1990s in bulk semiconductors, evidence of the condensation of excitons was inconclusive. A second wave of interest in collective phenomena in excitonic systems arose in the 21st century, when, due to advances in technology, researchers' interest shifted from bulk materials to nanostructures. It became possible to synthesize two-dimensional and quasi-two-dimensional structures, in which the motion of charge carriers is free in two directions and restricted in one direction. It is in two-dimensional systems, including structures with single and double quantum wells and quantum microcavities, that more convincing evidence of the formation of a collective state of these quasiparticles was obtained [17–23].

Nevertheless, despite the significant progress achieved in experimental and theoretical studies of collective and coherent effects in exciton systems, fundamental questions remained open about how the concept of Bose–Einstein condensate is generally applicable to experimentally studied structures. As is well known, condensation in ideal two-dimensional systems is impossible, but superfluidity of excitons is expected. The presence of potential fluctuations caused by structural imperfections, on the one hand, leads to the appearance of localized states, when the energy spectrum of excitons becomes discrete and condensation is formally possible, and, on the other hand, due to localization, superfluidity can be suppressed. Such a formulation of the problem has been discussed in the literature for two-dimensional [24–26] and one-dimensional [27, 28] systems; however, this analysis did not take into account another key feature of real systems — the finite lifetime of excitons and, accordingly, the need for optical or electrical pumping of the system. Recently, we have proposed a method that allows considering these circumstances within the framework of a unified model [29]. It was shown that the presence of disorder makes condensation possible, and the finite lifetime of excitons makes it difficult to thermalize excitons in a disordered system, leading to an additional limitation on the critical transition temperature. Note that the suppression of condensation due to the finite lifetime of excitons in bulk semiconductors was predicted in Ref. [30].

Excitons are interacting particles. The interaction may turn out to be quite strong, because of what other collective phases can be realized in exciton ensembles. In bulk semiconductors, the formation of an electron–hole liquid is possible, which can be collected in droplets [31–35]. In quasi-two-dimensional systems, the gas–crystal transition was predicted in the case where the repulsion between excitons is sufficiently long-range [36].

The purpose of this review is to present the main theoretical research of collective phenomena in exciton systems. Section 2 briefly discusses the Bose–Einstein condensation of excitons in bulk semiconductors, presents the main results for the spectrum of elementary excitations, analyzes the optical properties of the condensate, and discusses the role of disorder. Section 3 is devoted to collective phenomena in two-dimensional systems; the formally forbidden condensation in two-dimensional systems and the possibility of superfluidity of excitons are discussed. The same section presents the key results of the theory, which takes into account both disorder and the finite lifetime of excitons. The electron–hole liquid and the gas–crystal transition are briefly described in Section 4.

2. Bose–Einstein condensation of excitons in bulk semiconductors

2.1 Prediction

Theoretical predictions of the possibility of Bose–Einstein condensation for excitons [12–16] were made in the 1960s shortly after the pioneering discovery of large-radius excitons in the optical spectra of semiconductors by Gross and Karryev [37]. For noninteracting excitons with an isotropic parabolic dispersion law,

$$E_k = \frac{k^2}{2m}\,, \tag{2}$$

where k is the wave vector of the exciton, m is the mass of motion of the exciton as a whole, the density of particles accommodated by excited states $(E_k > 0)$ under the conditions of thermodynamic equilibrium is expressed as

$$N = \int f(E; T, \mu)\mathcal{D}_{3\mathrm{D}}(E)\,\mathrm{d}E\,. \tag{3}$$

Here,

$$\mathcal{D}_{3\mathrm{D}}(E) = \frac{\sqrt{m^3 E}}{\sqrt{2}\,\pi^2} \propto \sqrt{E} \tag{4}$$

is the density of states (here and below, we omit the factor associated with the possible spin and valley degeneracy of exciton states),

$$f(E; T, \mu) = \frac{1}{\exp\left[(E-\mu)/T\right] - 1} \tag{5}$$

is the equilibrium distribution function of the particles, T is the temperature of excitons, and $\mu \leqslant 0$ is their chemical potential. At a fixed concentration of excitons and decreasing temperature or a fixed temperature and increasing exciton concentration, the chemical potential increases, and at the critical temperature [3]

$$T_{\mathrm{c}}(N) = \frac{2\pi N^{2/3}}{\zeta^{2/3}(3/2)m} \approx 3.31\,\frac{N^{2/3}}{m} \tag{6}$$

becomes zero ($\zeta(x)$ is the Riemann ζ-function); see the inset in Fig. 1. At temperatures $T < T_{\mathrm{c}}(N)$ or at concentrations greater than the critical one (compare with estimate (1)),

$$N_{\mathrm{c}}(T) = \zeta\left(\frac{3}{2}\right)\left(\frac{mT}{2\pi}\right)^{3/2}, \tag{7}$$

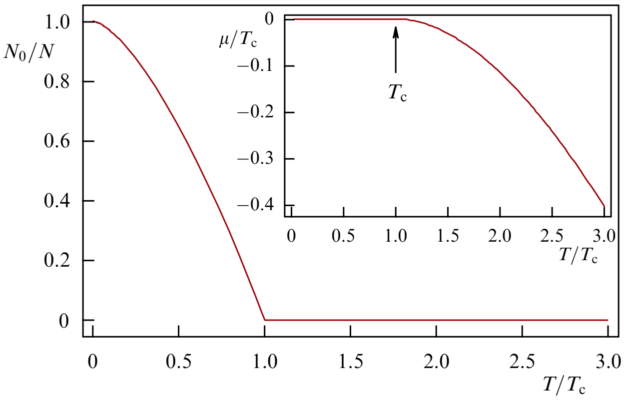

Figure 1. Fraction of excitons in the ground state as a function of temperature in the three-dimensional case, calculated using Eqn (8). The inset shows the temperature dependence of the chemical potential found from condition (3).

the state with $E = 0$ turns out to be macroscopically populated: the excitons that 'did not fit' into the excited states of the system condense in the state with zero energy and zero momentum. Their concentration is given by the formula

$$N_0 = N - N_c(T) = N\left[1 - \left(\frac{T}{T_c(N)}\right)^{3/2}\right]. \tag{8}$$

The temperature dependence of the condensate density is shown in Fig. 1; there is no condensate for $T \geqslant T_c$. Thus, excitons, like any other bosons, can form a Bose–Einstein condensate.

From the point of view of the theory of exciton condensation, the main questions are as follows:

(1) What is the spectrum of elementary excitations in an exciton condensate and to what extent are the Bose–Einstein statistics applicable to electron–hole pairs? In other words, what is the role of the exciton Bose gas imperfection?

(2) What are the manifestations of the exciton condensate in experiments?

(3) What is the role of the exciton system nonequilibrium and energy disorder in the effect of exciton condensation? Both of these factors are inevitable in experimentally studied semiconductor systems.

The basic difficulty from the point of view of theory lies in calculating the spectrum of elementary excitations in an exciton condensate. Possibilities of condensate manifestations in experiments are discussed in Section 2.3. The third issue will be discussed in detail below in Section 3, devoted to two-dimensional systems, where the disorder and nonequilibrium play a particularly important role. We now turn to an analysis of the effects associated with the exciton gas imperfection.

The spectrum of excitations in a Bose gas with weak repulsion was obtained by Bogoliubov [9]; for small wave vectors, it corresponds to the spectrum of sound:

$$\omega_k = sk, \tag{9}$$

where the effective velocity of sound s is determined by the force of interaction between bosons. Direct application of the Bogoliubov method to an exciton condensate encounters certain difficulties. As noted by Keldysh and Kozlov [38], for large-radius excitons, deviations from the Bose–Einstein statistics (associated with the fact that the commutator of the annihilation and creation operators of these composite quasiparticles contains contributions of $\sim Na_B^3$, where a_B is the Bohr radius of the exciton) manifest themselves at the same exciton densities as the effects of interparticle interaction. This difficulty can be overcome both by a detailed analysis of the four-fermion interactions (two electrons and two holes) [38, 39] and by introducing the effective amplitude f of exciton–exciton scattering with zero momentum transfer [15, 40]. Calculations show that the spectrum of elementary excitations has the form

$$\omega_k = \sqrt{\left(\frac{k^2}{2m}\right)^2 + \frac{4\pi f N}{m^2}\,k^2}\,. \tag{10}$$

For small k, the spectrum is linear (see Eqn (9)), and the velocity of sound is

$$s = \sqrt{\frac{4\pi f N}{m^2}}\,. \tag{11}$$

With a properly chosen scattering amplitude f, this expression fully corresponds to the answer for a weakly imperfect Bose gas [4, 9]. Here and below, it is assumed that $Nf^3, Na_B^3 \ll 1$; we also disregard the formation of exciton molecules (biexcitons). Naturally, Bose–Einstein condensation of excitons is only possible if they repulse, i.e., when $f > 0$. Generally, the interaction between the excitons has a complex character: depending on the orientation of their spins, both attraction and repulsion between these quasiparticles are possible, and their bound states (biexcitons) may arise. Hence, the collective states of excitons are not restricted to the Bose condensate; other possible phases are discussed in Section 4.

It is interesting to note that for small-radius excitons (Frenkel excitons) Eqn (10) for the spectrum remains valid, and the effective repulsion between the electron–hole pairs arises in accordance with the Pauli principle [16].

The spectrum of excitons in the form (10) meets the Landau superfluidity criterion [4]: in the plane (k, ω), the dependence ω_k lies above the straight line passing through the origin of coordinates with a nonzero slope. Therefore, the Bose–Einstein condensation of excitons in bulk semiconductors should be accompanied by a transition of excitons into a superfluid state [40], and the collective behavior of excitons will be described by the standard hydrodynamic equations for a superfluid liquid. The presence of weak disorder does not destroy the condensate, but leads to the damping of phonons $\gamma_k \propto k^4$ [41]. A detailed discussion of disorder effects is given in Section 3 for the case of the two-dimensional system of interest.

2.2 Optical properties

Excitons in semiconductors interact with the electromagnetic field: the absorption of light leads to the formation of excitons, and, vice versa, excitons have a radiative recombination channel.[1] Therefore, it is natural to look for manifestations of exciton condensation in the optical properties of semiconductors. The theory of the exciton condensate optical

---

[1] Generally speaking, in bulk crystals, exciton polaritons should be considered; however, as a rule, the anticrossing region of dispersion curves for light and excitons plays an insignificant role in the condensation effect.

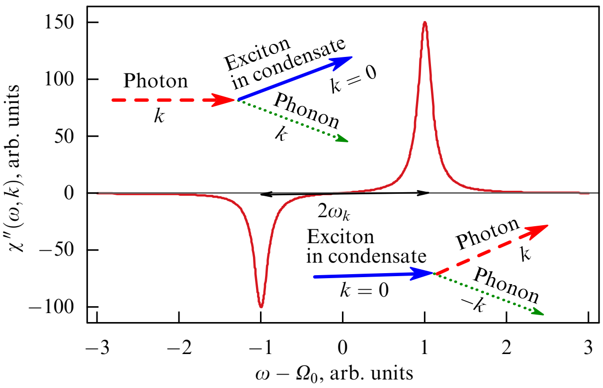

Figure 2. Imaginary part of the exciton condensate optical susceptibility. In the calculation, the delta-function peaks were replaced with Lorentz functions.

response was developed in [15]. It was shown that the imaginary part of the optical susceptibility of a crystal, in which the excitons have formed a condensed state, has the form

$$\chi''(\omega, \mathbf{k}) \propto (N_k + 1)\delta(\omega - \Omega_0 - \omega_k) - N_k \delta(\omega - \Omega_0 + \omega_k)\,. \qquad (12)$$

Here,

$$N_k = \frac{m^2 s^4}{2\omega_k(\omega_k + E_k + ms^2)} \qquad (13)$$

is the population of above-condensate states [4, 9, 15], and Ω_0 is the frequency of the exciton resonance (which includes the total energy shift due to exciton–exciton interaction). Formula (12) has a simple physical meaning: the first term corresponds to the absorption of a photon, due to which an exciton is created in the condensate together with a phonon, an above-condensate excitation. The second term describes the emission of a photon (amplification of an incident electromagnetic wave) due to stimulated annihilation of excitons. The appropriate susceptibility singularities are spaced apart in frequency by the doubled phonon energy $2\omega_k$. Dependence (12) plotted in Fig. 2 has two peaks corresponding to the absorption and gain of the electromagnetic field. We emphasize that, with an increase in the exciton concentration, the energy gap between the gain and absorption lines increases as the square root of the exciton concentration, and the line width for scattering by inhomogeneities decreases as the inverse square of the concentration due to the phonon character of the excitations and the Rayleigh law of their scattering [41].

2.3 Briefly about experiments

Note that, in a perfect crystal, single-photon recombination of a condensate exciton (with a wave vector $\mathbf{k} = 0$) is forbidden by the laws of conservation of momentum and energy. That is why, in optical transitions that contribute to the susceptibility (12), above-condensate excitations are also involved.[2] An interesting situation can be realized in semiconductors, where the ground state of the exciton is optically forbidden, e.g., for a para-exciton in copper oxide [42]. In this case, the exciton recombination from the condensate can be accompanied by emission of a host-lattice phonon, and the luminescence spectrum will be determined by the distribution function of excitons [11]. Moreover, the lifetime of 'forbidden' excitons can significantly exceed the time of their energy relaxation, which facilitates the achievement of a thermodynamic equilibrium state.

These circumstances motivated researchers to search for the condensation of excitons in bulk semiconductors [43–46] (see also reviews [47, 48]). Both spectroscopic studies aimed at detecting condensate luminescence [43, 44] and transport measurements aimed at searching for superfluidity were carried out [45, 49, 50]. However, the question of the discovery of a Bose–Einstein condensate in bulk $\mathrm{Cu_2O}$ (and in other bulk semiconductors) is still open. The effects of narrowing the luminescence line can be interpreted in alternative models that do not require condensate formation, but take into account the nonradiative recombination of excitons via the Auger mechanism [47, 51]. Some of the transport data can be described in terms of the phonon wind model — the drag of excitons by nonequilibrium phonons, arising due to intense sample heating [52, 53]. Much more convincing evidence of exciton condensation was obtained in two-dimensional systems, which will be discussed in Section 3.

3. Condensation of excitons in two-dimensional systems

3.1 Brief review of experimental systems

From the point of view of experiments on condensation of excitons, two-dimensional or quasi-two-dimensional semiconductor systems are the most attractive, in which the motion of charge carriers in the plane is free, and in the perpendicular direction, it is quantized. Two fundamentally different types of systems are being actively investigated: (1) structures with dipolar (spatially indirect) excitons (Fig. 3a,b) based on single or double quantum wells, or on van der Waals heterostructures with bilayer transition metal dichalcogenides [54, 55], where electrons and holes are separated in space; (2) structures with quantum microcavities, similar to those shown in Fig. 3c.

Dipolar excitons (Fig. 3a, b) have a significant radiative lifetime, since the overlap integral of the envelope wave functions of an electron and a hole, which describe the size quantization of charge carriers along the growth axis of the structure, is relatively small. As a result, the lifetimes of such excitons vary within a range from tens of nanoseconds to a few microseconds [56]. In such systems, excitons during their lifetime reach a state of thermodynamic equilibrium, which facilitates the realization of collective effects.

The situation is quite different in structures with microcavities, where a regime of strong coupling of excitons with photons trapped in microcavities is reached. In this case, new quasiparticles are formed — exciton polaritons [57, 58]. Their lifetime varies from unity to hundreds of picoseconds, depending on the sample [59], and are comparable to the thermalization time; therefore, exciton polaritons can be in a substantially nonequilibrium state. However, the small effective mass of exciton polaritons ($m \sim 10^{-4}\, m_0$, where m_0 is the mass of a free electron) allows reaching degeneracy in a

---

[2] In two-dimensional systems, the situation is different, since the absence of translational symmetry along the structure growth axis removes the law of the momentum normal component conservation. Such systems will be considered below in Section 3.

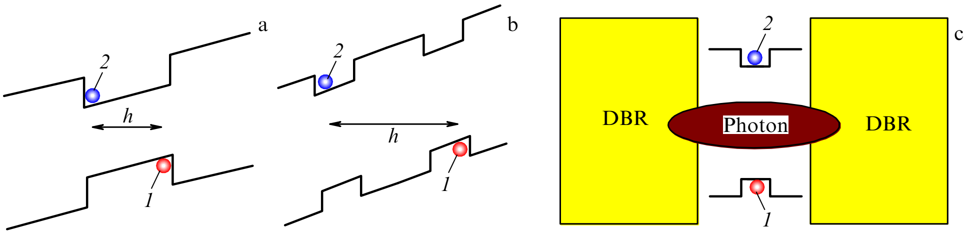

Figure 3. Basic systems in which the exciton condensation is experimentally studied: (a) a wide quantum well, (b) a double quantum well structure, (c) a structure with a microcavity containing a quantum well. It is assumed that an external or built-in electric field directed along the growth axis is applied to structures (a) and (b) to ensure spatial separation of charges. Parameter h is the characteristic distance between an electron and a hole along the normal to the plane of the wells. Red (*1*) and blue (*2*) circles denote a hole and an electron bound to an exciton by Coulomb interaction. DBR — distributed Bragg reflector.

two-dimensional Bose gas of polaritons, when

$$T_{2\mathrm{D}} \sim \frac{N}{m}\,, \tag{14}$$

even at room temperature ($T_{2\mathrm{D}} \sim 300$ K) and reasonable concentrations of quasiparticles $N \sim 10^{10} - 10^{11}$ cm^{-2} [57]. It is interesting to note that in structures with microcavities the condensation of photons can be observed, too [60].

3.2 Bose condensation and superfluidity in ideal two-dimensional systems

Before proceeding to the analysis of realistic structures, let us briefly dwell on the question of what exactly is understood by Bose–Einstein condensation in two-dimensional or quasi-two-dimensional systems, in which quasiparticles can only propagate in two dimensions. It is well known [4] that in perfect two-dimensional systems condensation is not possible. This statement is a result of the Mermin–Wagner theorem (sometimes referred to as the Mermin–Wagner–Hohenberg theorem or the Coleman theorem) [61–63] on the absence of phase transitions breaking continuous symmetries in systems with two or fewer dimensions (systems with an analytical spectrum) at a finite temperature. The appearance of a Bose–Einstein condensate leads to the appearance of a long-range order, which is characterized by correlations in a single-particle density matrix:

$$\rho(\mathbf{r}_1,\mathbf{r}_2) = \left\langle \psi^{\dagger}(\mathbf{r}_1)\psi(\mathbf{r}_2)\right\rangle\,, \tag{15}$$

where $\psi^{\dagger}(\mathbf{r})$ and $\psi(\mathbf{r})$ are the exciton creation and annihilation operators, and angle brackets denote averaging over an ensemble of particles. Condensation implies a nonzero limit [4, 9, 64, 65]

$$\lim_{|\mathbf{r}_1-\mathbf{r}_2|\to\infty} \rho(\mathbf{r}_1,\mathbf{r}_2) = N_{\mathrm{c}} \neq 0\,, \tag{16}$$

corresponding to nonzero first-order coherence in the system

$$g^{(1)} = \lim_{|\mathbf{r}_1-\mathbf{r}_2|\to\infty} g^{(1)}(\mathbf{r}_1,\mathbf{r}_2)\,, \qquad g^{(1)}(\mathbf{r}_1,\mathbf{r}_2) \equiv \frac{\rho(\mathbf{r}_1,\mathbf{r}_2)}{\sqrt{\rho(\mathbf{r}_1,\mathbf{r}_1)\,\rho(\mathbf{r}_2,\mathbf{r}_2)}}\,. \tag{17}$$

In two-dimensional and one-dimensional systems, $N_{\mathrm{c}} \equiv 0$ for $T > 0$; therefore, relation (16) is not valid, there is no long-range order, and, accordingly, there is no condensation.

It is easy to verify the absence of condensation in two-dimensional ideal systems without resorting to general statements. Instead, let us analyze the convergence of an integral similar to (3), which describes the filling of excited states. Since for particles with a parabolic law of dispersion in two dimensions the density of states $\mathcal{D}_{2\mathrm{D}}$ does not depend on the energy, then the integral

$$\int_0^{\infty} f(E;T,\mu)\mathcal{D}_{2\mathrm{D}}\,\mathrm{d}E \sim \ln\left(\frac{T}{|\mu|}\right)$$

diverges at $\mu \to 0$. This means that the excited states of the system can accommodate an unlimited number of bosons; therefore, the macroscopic population of the state with $\mathbf{k} = 0$ is impossible at finite temperatures. Condensate can be formed only at $T = 0$.

We emphasize that the above reasoning applies only to an ideal system, possessing translation invariance. A natural opportunity to allow condensation is to create a potential well (trap) for particles, in which the ground state of the particles is separated from the excited states by the energy gap ΔE [66].[3] In this case, the sum of the occupation numbers of excited states remains finite at any value of the chemical potential, and condensation (in the sense of ground state macroscopic population) turns out to be possible. Let us make sure of this with a simple example. Consider a potential well so small that it contains only one energy level of size-quantization. A more general case is considered below in Section 3.4. Then, the population of excited states with $E > 0$ is described by a converging integral (the maximum permissible value being $\mu = -\Delta E$)

$$\int_0^{\infty} \frac{\mathcal{D}_{2\mathrm{D}}\,\mathrm{d}E}{\exp\left[(E+\Delta E)/T\right]-1} < +\infty\,.$$

The rest of the particles, as in a three-dimensional system, condense in the ground state, in this case at the level of size-quantization in the trap. In the pioneering work [18, 19], this very experimental configuration was used, and the traps were formed due to large-scale spatial variations of the potential in the system. The thermodynamic properties of bosons in a trap are considered in Section 3.4.

There is also another possibility of implementing collective effects in a two-dimensional system of excitons. Two-dimensional Bose particles with weak repulsion at sufficiently low temperatures can transit to the superfluid state [4, 67–70]. The corresponding transition, called the Kosterlitz–Thouless or Berezinskii–Kosterlitz–Thouless (BKT) transition, is not strictly a phase transition; however, the boson system at temperatures $T < T_{\mathrm{BKT}}$ and $T > T_{\mathrm{BKT}}$ behaves differently,

---

[3] We recall that traps are used to observe the condensation of atoms [7, 8].

where T_{BKT} is the transition temperature. When $T < T_{\mathrm{BKT}}$, the single-particle density matrix (15) decreases slowly according to the power law; when $T > T_{\mathrm{BKT}}$, it decreases exponentially. The temperature of the BKT transition and the degeneracy temperature coincide with the accuracy of a logarithmic factor, which depends on the concentration of bosons and the interaction magnitude [4].

Lozovik and Yudson [71, 72] drew attention to the possibility of superfluidity of excitons in two-dimensional and quasi-two-dimensional systems. Note that at zero temperature all excitons are naturally in the ground state with $k = 0$, and the spectrum of elementary excitations for small k is given, as in the three-dimensional case, by formula (9): $\omega_k = sk$ (we consider the case of repulsion between excitons; see also [73–75]). Such a spectrum satisfies the Landau criterion of superfluidity [4]; therefore, a two-dimensional exciton gas with a weak repulsion is superfluid. At a finite temperature $T < T_{\mathrm{BKT}}$, the density of the superfluid component of the exciton gas is less than that at $T = 0$, and at $T \geqslant T_{\mathrm{BKT}}$, the superfluid component completely disappears.

Thus, collective effects can be expected in two-dimensional exciton systems: first, Bose–Einstein condensation in the presence of energy disorder or traps leading to localization of particles, and second, superfluidity, which, however, can be suppressed due to the presence of potential fluctuations.[4] The competition between these two effects results in a nontrivial phase diagram including superfluid, delocalized, and localized phases [26]. There is one more feature of excitons: these quasiparticles have a finite lifetime; therefore, the implementation of collective effects requires the presence of pumping. It was shown in [29] that the finite lifetime of excitons complicates the thermalization of excitons in a disordered system and leads to an additional restriction imposed on the critical transition temperature.

Next, we will consider the thermodynamic properties of two-dimensional excitons, taking into account disorder and the finite lifetime. Then, the effects of interaction will be discussed, as well as fluctuation effects associated with the nonequilibrium state of the system caused by the competition of the pump and the finite lifetime.

3.3 Thermodynamics of two-dimensional excitons and effects of disorder

We will consider two-dimensional systems with single or double quantum wells similar to those studied in [18, 56, 76, 77], where the disorder can be caused, for instance, by monolayer fluctuations of the well width (Fig. 4a). The regions where the well is wider effectively localize the exciton [78, 79]. Such areas of localization are potential wells for the lateral motion of excitons. A similar situation may be implemented in other two-dimensional or quasi-two-dimensional exciton systems and exciton–polariton systems, e.g., in the presence of repulsing impurities, the chaotic distributions of which in the structure plane can induce the formation of potential wells. For exciton polaritons, the fluctuations of the cavity width may also serve as a source of energy disorder [57].

In a two-dimensional disordered system, all single-particle states are localized [80]. We will consider the situation where the energy spectrum of localized states is limited from below [29]. In what follows, for simplicity, we will count the energies from the edge of the spectrum $E = 0$. Near the edge of the spectrum, the density of exciton states can be presented in the form [81, 82]

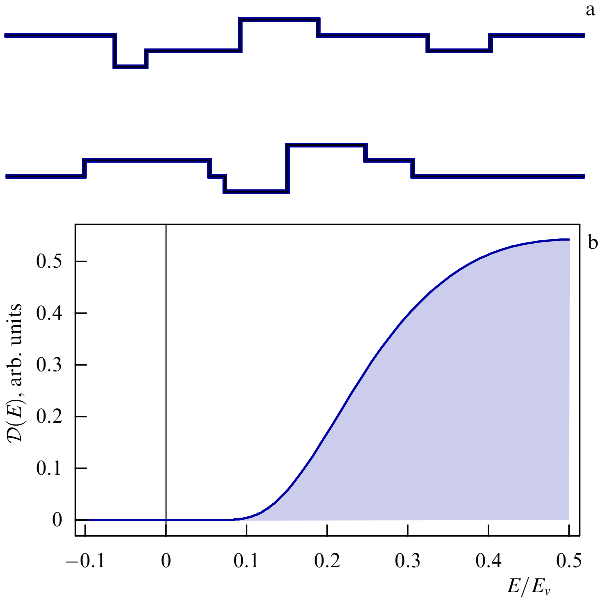

Figure 4. (a) Schematic representation of a quantum well with disorder due to fluctuations in the well width. (b) Density of states (18).

$$\mathcal{D}(E) = \begin{cases} \dfrac{N_{\mathrm{p}} E_v}{E^2} \exp\left(-\dfrac{E_v}{E}\right), & E > 0\,, \\ 0\,, & E < 0\,. \end{cases} \tag{18}$$

Here, E_v is the characteristic width of the band of localized states, and N_{p} is the concentration of wells. The density of states is normalized by the relation

$$\int_0^{\infty} \mathcal{D}(E)\, \mathrm{d}E = N_{\mathrm{p}}\,, \tag{19}$$

which corresponds to taking into account only one localized state per potential well. The exponential factor $\exp(-E_v/E) = \exp(-\pi R^2 N_{\mathrm{p}})$ in the density of states describes the probability of finding a well of radius R with the exciton localization energy $E = (mR^2)^{-1}$, where m is the mass of motion of the exciton as a whole. Here, we omit the factor of the order of unity, which depends on the geometry of the well. In the well model, $E_v = \pi N_{\mathrm{p}}/m$, and the prefactor in Eqn (18) can be easily obtained using the relation $R\,\mathrm{d}R = -(2mE^2)^{-1}\,\mathrm{d}E$. The density of states is shown in Fig. 4b. Relation (18) for the density of states is valid for not too high energies $E \lesssim E_v$, but if $E \gg E_v$, then the exponent becomes of the order of unity and the density of states ceases to depend on the exciton energy. However, such energies are insignificant for discussing the condensation of excitons.

The vanishing of the density of states at the edge of the spectrum is because the presence of a state at $E \to 0$ would require the existence of a well of infinitely large radius R; the probability of finding such a well is negligibly small. This is the key difference between a disordered two-dimensional system and an ideal one, where the density of states at the edge of the spectrum undergoes a jump. The fact that $\mathcal{D}(E)$

---

[4] In this section, we consider the interaction between excitons to be fairly short-range. The presence of a long-range part in the exciton–exciton interaction potential leads to a number of additional effects, discussed in Section 4.

becomes zero at $E \to 0$ opens up the possibility of Bose condensation of excitons in two-dimensional systems. First, let us analyze this possibility within the framework of the thermodynamic approach, assuming the lifetime of excitons to be so long that the particles are described by the equilibrium distribution function (5). It can be shown that the critical temperature $T_{\rm c}$ and the concentration $N_{\rm c}$ of excitons are related as [29]

$$N_{\rm c} = \int_0^{\infty} f(E; T_{\rm c}, 0)\mathcal{D}(E)\,{\rm d}E\,. \qquad (20)$$

The concentration of wells is considered quite high, the temperature is low, and the density of excitons is low, so that the interaction between the particles can be ignored. With a logarithmic accuracy, the condensation temperature can be represented as

$$T_{\rm c} \approx \frac{4E_v}{\ln^2\left(\sqrt{\pi}\,N_{\rm p}/N_{\rm c}\right)}\,. \qquad (21)$$

The logarithmic factor in (21) is assumed to be large, so that $T_{\rm c} \ll E_v$; in this case, the critical temperature logarithmically depends on the concentration of excitons. This is due to the exponentially low density of states at $E \to 0$. Note that the critical temperature $T_{\rm c}$, determined by Eqn (21), turns out to be significantly higher than the degeneracy temperature of the ideal two-dimensional Bose gas without disorder, $T_{\rm 2D} \sim N_{\rm c}/m$. Such a seemingly unexpected relationship between the degeneracy temperature and the condensation temperature is a consequence of exciton disorder. Indeed, at $T \sim T_{\rm c}$, the average distance between the occupied wells is large, and the overlapping of de Broglie waves of excitons is insignificant, but inside a given well the ground state is occupied by a macroscopically large number of excitons. Figure 5 shows the dependence of the critical temperature on the density, found by exact calculation from Eqn (20) (solid curve), and the logarithmic asymptotic behavior (21) (dotted line).

Thus, the presence of disorder leads to Bose–Einstein condensation of excitons in two-dimensional systems, which is quite analogous to the formation of condensate in traps [66, 83, 84].

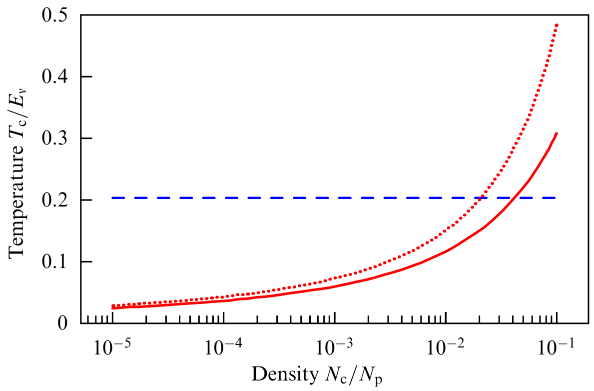

Figure 5. Critical temperature of Bose condensation of excitons depending on density. Solid curve — exact calculation by formula (20), dotted curve — asymptotic expression (21). The dashed horizontal line shows the temperature $T_{\rm k}$ (29) corresponding to the lower bound of condensation temperature due to the finite lifetime of particles, calculated at $N_{\rm p}/\varkappa^2 = 0.3$, $w_0\tau_0 = 10^7$ (see Section 3.5 for details). (From [29].)

3.4 Statistics of bosons in a single trap

To complete the picture, we present a brief thermodynamic description of the statistics in a single potential well (trap). For a discrete spectrum characterized by a set of energy levels E_i, the relationship between the number of particles and the chemical potential is similar to Eqn (3):

$$N = \sum_i f(E_i; T, \mu)\,. \qquad (22)$$

Naturally, the chemical potential μ for any finite N lies below the ground state of the bosons, $\mu < E_0$, and approaches E_0 when $N \to \infty$. Excited states of the system with energies $E_i > E_0$ can accommodate only a limited number of particles N', since the sum $\sum_{i \neq 0} f(E_i; T, E_0) \equiv N'$ converges. When $N > N'$, the remaining number $N - N'$ of particles turns out to be in the ground state.

Following Ref. [66] (see also [85]), let us briefly analyze the statistics of excitons in a trap described by a harmonic oscillator potential — a harmonic trap. The simplest case corresponds to an equidistant set of energy levels

$$E_i = \omega\left(i + \frac{1}{2}\right), \quad i = 0, 1, \ldots\,. \qquad (23)$$

Here, ω is the harmonic frequency corresponding to the parabolic potential of the trap. Such a trap is referred to as a one-dimensional trap [66]. Note that such traps are often used to describe condensation in two-dimensional extended systems [66], since the density of states, averaged over the energy band $\Delta E \gg \omega$, does not depend on energy. Let us define the critical temperature $T_{\rm c}$ for a given number of excitons N in such a way that, at $T = T_{\rm c}$, the population of the ground state is equal to the total population of all other states of the trap. In other words, at a temperature equal to the critical one,[5]

$$f(E_0; T_{\rm c}, \mu) = \frac{1}{\exp\left[(E_0 - \mu)/T_{\rm c}\right] - 1} = \frac{N}{2}\,, \quad N' = \frac{N}{2}\,.$$

The dependence $T_{\rm c}(N)$ is shown in Fig. 6a. With logarithmic precision, $T_{\rm c} = \omega N \ln N$, which coincides with the Bose gas degeneracy condition in a one-dimensional harmonic potential. Figure 6b shows the temperature dependence of the proportion of excitons in the ground and excited states for the total number of excitons $N = 10$ and $N = 100$. With increasing N, the curves become slightly sharper at $T > T_{\rm c}(N)$. The transition becomes more pronounced in a three-dimensional harmonic trap (see inset in Fig. 6b).

Despite the fact that such a behavior of the ensemble of bosons can be called condensation in the wide sense of this notion, strictly speaking, with finite N the phase transition in the system is absent, and the level populations (as well as thermodynamic parameters, e.g., heat capacity) behave smoothly, depending on temperature. For $N \to \infty$, the transition turns out to be abrupt, but the transition temperature $T_{\rm c}(N)$ also tends to infinity.

3.5 Role of finite lifetime

Let us now return to a two-dimensional disordered system. The consideration in Section 3.3 does not take into account an important circumstance, namely, excitons, like other quasi-

---

[5] In Ref. [66], a different condensation criterion was used, which coincides with the one used here by an order of magnitude.

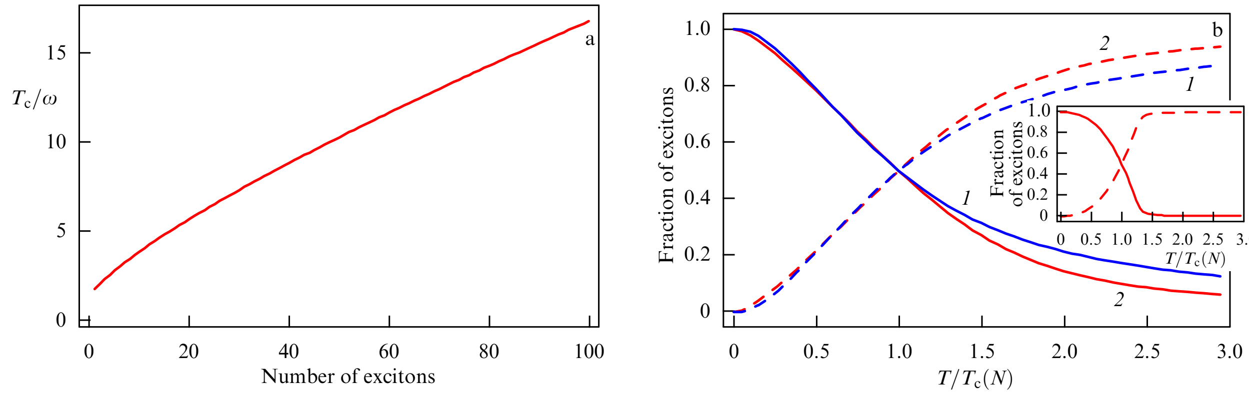

Figure 6. (a) Dependence of the critical exciton condensation temperature in a one-dimensional harmonic trap on the number of excitons N. (b) Fraction of excitons in the ground state (solid curves) and excited states (dashed curves) of a one-dimensional trap as a function of temperature, scaled to the temperature of condensation, for $N = 10$ (blue curves *1*) and $N = 100$ (red curves *2*). The inset shows similar dependences for a three-dimensional trap at $N = 200$. ω is the frequency corresponding to the parabolic potential of the trap (see (23)).

particles, have a finite lifetime. Therefore, the possibility of describing an ensemble of excitons by the equilibrium Bose–Einstein distribution function (5) requires an analysis of the competition between the processes of thermalization of excitons and their elimination from the system. In particular, as shown in Ref. [30], the finite lifetime of an exciton in a bulk semiconductor gives rise to a lower bound for the condensate concentration even at $T = 0$. In a two-dimensional disordered structure, the low density of low-energy states (18) hinders relaxation, which imposes restrictions on the exciton condensation temperature [29].

Figure 7 illustrates exciton kinetics in a disordered system. Let us introduce the lifetime of an exciton τ_0, caused by the processes of both radiative and nonradiative recombination. We will ignore its dependence on the exciton energy. The transitions between localized exciton states in the wells are characterized by the probability per unit time of hopping between the wells with energies E and E', separated by distance r from each other [86–89]:

$$w(E \to E', r) = w_0 \exp(-2\varkappa r) \begin{cases} 1\,, & E' \leqslant E\,, \\ \exp\left(\dfrac{E - E'}{T}\right), & E' > E\,. \end{cases} \tag{24}$$

Here, $\varkappa$ is the inverse length of the sub-barrier tunneling between the wells, and w_0 is a parameter determined by the specific form of the wave functions of localized excitons and by the mechanism of exciton–phonon interaction, where the energy dependence of w_0 is ignored. The exponential factor $\exp[(E - E')/T]$ at $E' > E$ describes the contribution from the hops upward in energy with absorption of a phonon. We denote by G the rate of excitons entering the wells due to the pumping and energy relaxation of excitons in the region of states with energies $E \gtrsim E_v$.

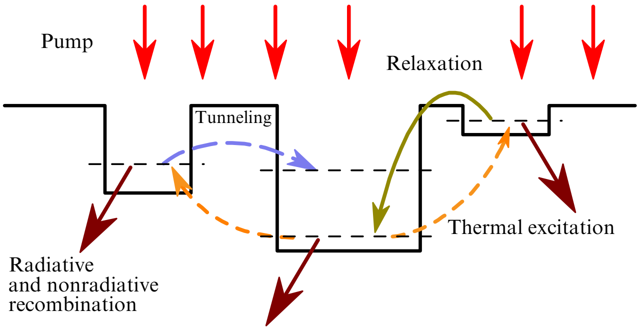

Figure 7. Schematic representation of the exciton kinetics in potential wells. The processes of recombination, energy relaxation, tunneling, and thermal excitation are shown.

In disordered systems, the rates of transitions between localized states $w(E \to E', r)$ have an exponentially wide distribution, which does not allow introducing a single energy relaxation time for excitons [86, 90]. However, due to this exponential scatter, all wells can be divided into two categories: those that the exciton can leave during its lifetime, and those from which the departure time is greater than the time τ_0. The latter will be referred to as *traps*. The probability that a well with energy E is a trap is described by the expression

$$P_{\rm tr}(E) = \exp\left[-K(E)\right], \tag{25}$$

where

$$K = \int_{w(E \to E', r)\tau_0 > 1} {\rm d}E' \, {\rm d}r \, 2\pi r \, \mathcal{D}(E')\,. \tag{26}$$

Formulas (25) and (26) describe the probability that near a given well there are no such wells to which the exciton could jump during its lifetime. For $E \to 0$, the probability that a given well is a trap tends to unity, $P_{\rm tr}(0) = 1$. The release of excitons from traps occurs only due to recombination, and the rate G of excitons entering the traps can be considered independent of localization energy in a rough but sufficient for a qualitative analysis approximation. Thus, the population of the traps does not depend on the energy E. As a result, the energy distribution function of excitons in the traps takes the form

$$f_{\rm tr}(E) = G\tau_0 P_{\rm tr}(E)\,, \tag{27}$$

which differs significantly from equilibrium distribution (5). In this case, the traps turn out to be in no way connected, and the phases of the exciton functions in them are uncorrelated. This means that the criterion for the condensation of excitons in a disordered system must be modified.

The analysis carried out in Ref. [29] shows that the function $P_{\rm tr}(E)$ falls rather sharply with an increase in the

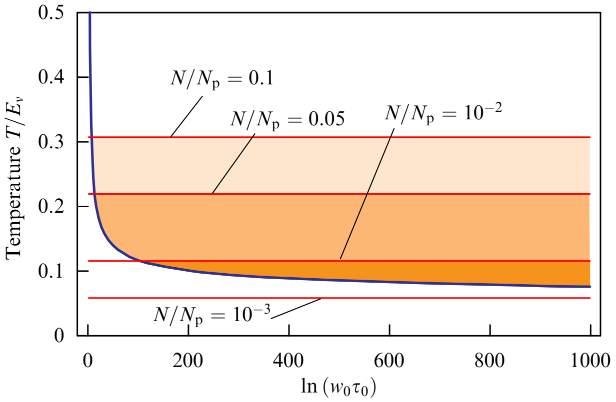

Figure 8. Diagram of exciton states in a disordered system. The horizontal straight lines show the condensation temperature for various values of $N/N_{\rm p}$, calculated using Eqn (20). The curve shows temperature $T_{\rm k}$ in Eqn (29), calculated at $N_{\rm p}/\varkappa^2 = 0.3$. The shaded areas show the parameters for which the condensation is possible at a given density N: $T_{\rm k} < T < T_{\rm c}(N)$. (From [29].)

exciton energy, and it is possible to introduce the characteristic critical energy $E_{\rm c}$, above which there are practically no traps:

$$K(E_{\rm c}) = 1\,. \tag{28}$$

This energy may be associated with the edge of the 'hopping mobility' of excitons. If the edge of the hopping mobility of excitons falls into the thermal band $E_{\rm c} \lesssim T$, then the restrictions (27) on the distribution function of excitons associated with their finite lifetime are insignificant, and the condensation of excitons can be assumed to be possible. If the temperature is sufficiently low, $T \ll E_{\rm c}$, then the distribution function of excitons is strongly nonequilibrium, and it is impossible to talk about their Bose–Einstein condensation in the strict sense of this term. Thus, the condensation of excitons is possible at a temperature

$$T > T_{\rm k} \equiv E_{\rm c} = \frac{E_v}{\ln\left[(\pi N_{\rm p}/4\varkappa^2)\ln^2(w_0\tau_0)\right]}\,. \tag{29}$$

For excitons in a disordered system, the diagram of states in the coordinate axes 'lifetime logarithm–temperature', calculated in [29] with restriction (29) taken into account, is shown in Fig. 8.

3.6 Interaction and superfluidity of excitons

Until now, we have assumed that there is no interaction between excitons. This is acceptable under the condition that the energy shift of the exciton level remains small in comparison with the separation between the levels in the well. In a well of radius R for exciton density N, the energy level shift because of exciton–exciton interaction can be estimated in the single-scattering approximation as

$$\delta E \equiv \mathcal{E}_R - E_R = \mathcal{T}N\,, \quad \mathcal{T} = \frac{2\pi}{m}\,\frac{1}{\ln(E_0/\mathcal{E}_R)}\,. \tag{30}$$

Here, $E_R = (mR^2)^{-1}$ is the size-quantization energy in a well,[6] $\mathcal{E}_R$ is the energy taking into account the interparticle interaction, $\mathcal{T}$ is the amplitude of the exciton–exciton scattering. The interaction is assumed to be short-range, we assume $\mathcal{T} > 0$, which corresponds to the repulsion between excitons. The situation of a more complex exciton–exciton interaction, in particular, dipole–dipole repulsion, is analyzed in Section 4. As is known, in a two-dimensional system at low energies, the amplitude $\mathcal{T}$ has a logarithmic singularity [92]; correspondingly, the cutoff energy $E_0 \sim 1/(ma^2)$ is introduced into Eqn (30), where a is the radius of the exciton–exciton interaction potential. For the exchange interaction between excitons, a is of the order of the Bohr radius of the exciton, and E_0 is of the order of the exciton binding energy [93]. Accordingly, in Eqn (30), the logarithmic factor is considered large:

$$\ln\left(\frac{E_0}{\mathcal{E}_R}\right) \gg 1\,, \quad \frac{m}{2\pi}\ln\left(\frac{E_0}{\mathcal{E}_R}\right) \gg \Gamma^{-1}\,,$$

where Γ is the bare interaction constant. Thus, with a logarithmic accuracy, the solution to Eqn (30) is written in the form

$$\mathcal{E}_R - E_R = \frac{2\pi N}{m}\,\frac{1}{\ln\left[mE_0/(2\pi N)\right]} \sim \frac{2\pi N}{m}\,\frac{1}{\ln\left[1/(Na^2)\right]}\,. \tag{31}$$

The requirement for a small energy shift corresponds to restriction

$$NR^2 \ll \ln\left(\frac{mE_0}{2\pi N}\right)\,. \tag{32}$$

Thus, at low concentrations, the wave functions of excitons, when they are distributed over virtually independent wells, are correlated within each well.

With an increase in the concentration of excitons, condition (32) is violated and the distribution of excitons over a random potential becomes determined by the competition of potential fluctuations that localize excitons and by the repulsion of excitons from each other, which leads to an effective distribution of excitons over a large area. As a result, the random potential is effectively screened (a similar situation takes place in the three-dimensional case [41]). Qualitatively, the following behavior of an ensemble of excitons can be expected: an increase in the concentration of excitons in the wells leads to a blue shift of the energy level in these wells, and in deeper wells, where the concentration of particles is higher, the shift also appears to be larger (see the schematic illustration in Fig. 9). This leads to effective equalization of energies $\mathcal{E}_R$ in wells with different radii R. If for wells with radii R and R' the energy difference becomes of the order of or less than the tunnel coupling constant between the wells $J_{RR'}$,

$$|\mathcal{E}_R - \mathcal{E}_{R'}| \lesssim J_{RR'}\,,$$

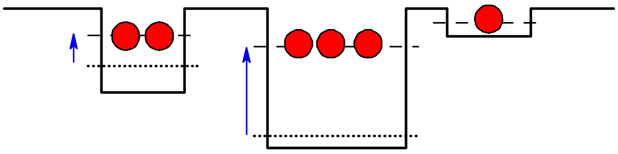

Figure 9. Illustration of the energy shifts of exciton levels in wells. In wells with a larger number of excitons, the shift turns out to be larger.

---

[6] As above, we do not take into account the numerical factor associated with the shape of the well; calculations for specific well shapes are given, e.g., in Ref. [91].

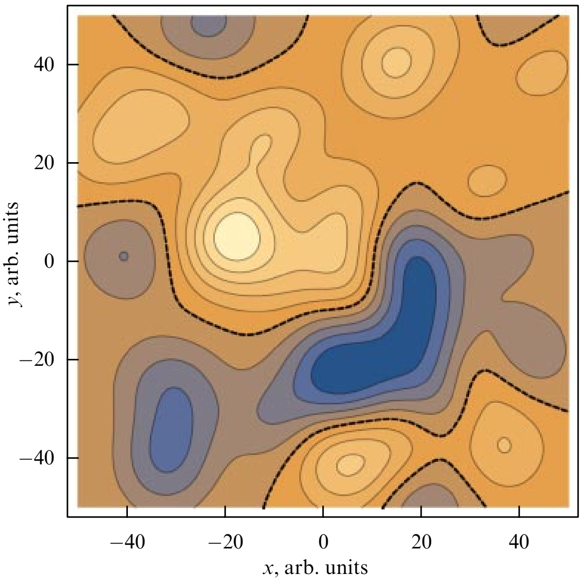

Figure 10. Schematic illustration of the percolation effect in a random potential $V(\mathbf{r})$. The dashed line shows the level of leakage V_c. At $\mu > V_c$ the potential wells turn out to be coupled.

then the exciton condensates in different wells begin to unite efficiently. In this case, the synchronization of condensates becomes possible; their wave functions turn out to be correlated on the scale of coupled wells [94–96]. Thus, with an increase in the concentration of excitons, the interaction between them leads to the spread of coherence over a larger and larger area. Ultimately, all the wells become occupied, and the 'extra' excitons fill the entire space (compare with the scenario considered in [97]). The picture becomes the same as in the absence of impurities. Excitons are distributed in space with such a concentration $N(\mathbf{r})$ that allows complete screening of the random potential $V(\mathbf{r})$. Namely, their chemical potential,

$$\mu = \mathcal{T}N(\mathbf{r}) + V(\mathbf{r}) \quad \text{for} \quad \sqrt{\mathcal{T}Nm} \gg V^{-1}\left|\frac{\partial V}{\partial r}\right|, \tag{33}$$

does not depend on the coordinate [4, 98]. The situation in this case is completely analogous to the classical percolation problem — the fluid flow in a potential relief $V(\mathbf{r})$ [90, 99]. The chemical potential at which the wells are coupled corresponds to the percolation threshold in the system $\mu = V_c$ [97] (Fig. 10). If the concentration of excitons N is large enough so that $\mu \gg V_c$, then the interacting excitons can be described as an ideal (superfluid) liquid [4, 29, 40, 100]; however, even at zero temperature, there are fluctuations in the exciton system due to pump fluctuations (see Section 3.7 below).

Note that the complete 'phase diagram' of weakly interacting bosons in a two-dimensional disordered system under conditions of thermodynamic equilibrium can include, in addition to the localized and superfluid phases, the phase of a normal liquid [26]. The possibility of delocalization of bosons due to the interaction at temperatures exceeding the degeneration temperature T_{2D} is associated with the appearance of resonant pairs of two-particle states, the matrix element of the interaction between which exceeds the difference between their energies. This leads to the many-particle localization–delocalization transition [26–28, 101] (see also the analysis of the transition between localized and superfluid states in Ref. [24]). We note, however, that Ref. [26] considers the states of bosons with energies $E \gtrsim E_v$, i.e., the effects associated with the density tails of the Lifshitz states (18) are disregarded, whereas here (see also [29]) the main focus is on the occupation of low-energy states as well as the regime of a sufficiently high density, when the random potential is screened.

3.7 Fluctuations in a nonequilibrium exciton condensate

Let us now proceed to analyzing the fluctuation effects in exciton condensates due to the presence of energy disorder and pump fluctuations. First, we will briefly consider the effects associated with the random potential $V(\mathbf{r})$ at zero temperature, ignoring also the fluctuations associated with the kinetics of excitons. On a qualitative level, the presence of disorder leads to the escape of particles from the condensate state [41]. The depletion of the condensate can be understood by representing, according to (33), the single-particle density matrix (15) in the form

$$\rho(\mathbf{r}_1, \mathbf{r}_2) = N\left\langle \exp\left[\mathrm{i}\big(\varphi(\mathbf{r}_1) - \varphi(\mathbf{r}_2)\big)\right] \right.$$
$$\left. \times \left[\left(1 - \frac{V(\mathbf{r}_1)}{\mu}\right)\left(1 - \frac{V(\mathbf{r}_2)}{\mu}\right)\right]^{1/2}\right\rangle,$$

where $N = \mu/\mathcal{T}$ is the average concentration of excitons, and $\varphi(\mathbf{r})$ is the phase of the wave function. It is easy to verify that at large distances, when $|\mathbf{r}_1 - \mathbf{r}_2|$ exceeds the correlation length of the potential, for the single-particle correlator the following estimate is obtained:

$$\rho(\mathbf{r}_1, \mathbf{r}_2) \leqslant N\left(1 - \frac{\langle V^2 \rangle}{4\mu^2}\right). \tag{34}$$

Expression (34) is true for smooth weak disorder, when $\sqrt{\langle V^2 \rangle} \ll \mathcal{T}N$. Thus, the random potential leads to a decrease in the number of particles in the condensate, as well as to a decrease in the superfluid fraction of excitons in the system [102–106]. This leads to a decrease in the critical temperature of the BKT transition in comparison with the ideal case.

The presence of a random potential also leads to the damping of Bogoliubov excitations due to their Rayleigh scattering by disorder. The calculation shows that for quanta with a wavelength exceeding the correlation length of the condensate, the decay rate due to the disorder in systems of dimensions D = 2 and 3 is described by the law [29, 41]

$$\gamma_k \propto \begin{cases} k^3, & \mathrm{D} = 2, \\ k^4, & \mathrm{D} = 3. \end{cases} \tag{35}$$

Thus, sound excitations of the condensate with small wave vectors $k \to 0$ have an arbitrarily long lifetime in relation to scattering by disorder.

Let us now describe the fluctuation effects arising in exciton condensates due to the finite lifetime of quasiparticles and the presence of pumping. First, let us consider fluctuations in the number of particles of condensate N, caused by random processes of excitons entering and leaving the ground state. Here and below, the area of the structure is considered to be unity; therefore, we do not make a distinction between the density of particles and their number. It is easy to show that

$$\frac{dN}{dt} = W_{\text{in}}(1+N) - \left(\frac{1}{\tau_0} + W_{\text{out}}\right) N\,, \tag{36}$$

where W_{in} is the rate of entering the ground state due to the processes of exciton generation and energy relaxation, the factor $1+N$ is due to the Bose statistics of excitons, and W_{out} is the rate of departure to the excited states due to thermal excitation. The stationary number of particles in the ground state can be written as

$$\langle N \rangle = \frac{W_{\text{in}}}{\tau_0^{-1} + W_{\text{out}} - W_{\text{in}}}\,. \tag{37}$$

Analysis of the terms responsible for the entering and leaving processes in the kinetic equation shows that the stability condition $\tau_0^{-1} + W_{\text{out}} - W_{\text{in}} > 0$ is satisfied [107]; therefore, $\langle N \rangle > 0$. The dynamics of fluctuations $\delta n = N - \langle N \rangle$ are described by Eqn (36) with N replaced with $\langle N \rangle + \delta n$. Therefore, the relaxation of fluctuations in the number of particles is characterized by the correlation time τ_N:

$$\frac{1}{\tau_N} = \frac{\tau_0^{-1} + W_{\text{out}}}{1 + \langle N \rangle}\,. \tag{38}$$

The deceleration of the dynamics of fluctuations is a remarkable property of Bose systems: stimulated scattering of particles with a transition to the ground state supports their fluctuations [107]. In accordance with expression (38), the greater the number of excitons in the ground state, the longer the fluctuations in their number persist.

Calculations of the root-mean-square fluctuation of the number of excitons in condensate because of competition between the processes of quasiparticle in- and outflow require the calculation of the full distribution function of excitons. The corresponding analysis [108, 109] shows that at $\langle N \rangle \gg 1$ the fluctuations in the ensemble of excitons are suppressed and

$$\langle \delta n^2 \rangle = \langle N \rangle\,. \tag{39}$$

In terms of quantum optics, this relation corresponds to the second-order coherence equal to unity, $g^{(2)} = 1$, i.e., the so-called coherent statistics of excitons. This corresponds to the fact that, for sufficiently large N, the exciton condensate, even in the presence of random processes of in- and outflow of particles, can be described as the classical field $\psi(\mathbf{r}, t)$. This is similar to how in a conventional laser the processes of stimulated emission into the laser mode suppress fluctuations in the number of photons in the cavity, which allows the laser to be described quasi-classically in terms of the field $\mathbf{E}(\mathbf{r}, t)$ [110]. The corresponding equation for the exciton field can be written in the form (cf. [111, 112])

$$\begin{aligned} &\mathrm{i}\,\frac{\partial \psi}{\partial t} + \frac{1}{2m}\,\Delta\psi - \mathcal{T}|\psi|^2\psi - V(\mathbf{r})\psi + \frac{\mathrm{i}}{2}(\tau_0^{-1} + W_{\text{out}} - W_{\text{in}})\psi \\ &\quad = \mathrm{i}\,j(\mathbf{r}, t)\,. \end{aligned} \tag{40}$$

On the right-hand side of Eqn (40), we took into account the effective current $j(\mathbf{r}, t)$, which describes the spontaneous processes in the system (in particular, pump fluctuations by analogy with Langevin forces in the noise theory). Equation (40) is nothing but the Gross–Pitaevskii equation for the wave function of the exciton condensate $\psi(\mathbf{r}, t)$, supplemented by contributions describing the in- and outflow of particles from the condensate. The contribution

$$\propto W_{\text{in}}\psi$$

has the meaning of the gain in the laser terminology, and the contribution

$$\propto (\tau_0^{-1} + W_{\text{out}})\psi$$

describes the loss. We note that, in a number of papers (see [113, 114]), Eqn (40) is supplemented by a nonlinear term responsible for the escape, $-\mathrm{i}\Gamma|\psi|^2\psi$, which stabilizes the number of particles in the condensate. Strictly speaking, this is not required if we write separately the kinetic equations for the occupation numbers of excited states of excitons, which, as noted above, automatically imposes restrictions on W_{in} and W_{out} corresponding to the physical condition $\tau_N > 0$ in (38). In the case of resonant optical excitation of excitons or exciton polaritons, it is necessary to include in effective current $j(\mathbf{r}, t)$ a contribution proportional to the external electric field applied to the system [112, 115, 116].

Note that the macroscopic population of the ground state $\langle N \rangle \gg 1$ leads to a corresponding increase in the temporal coherence of the first order in the exciton ensemble. The essence of the result can be seen from formula (40), which shows that when we ignore the interaction, $\mathcal{T}|\psi|^2 \to 0$, and the spatial inhomogeneity of the system, $V(\mathbf{r}) \to 0$, the damping of the fluctuation $\delta\psi(\mathbf{r}, t)$ is described by the correlation time

$$\tau_{\text{c}} = 2\tau_N \propto \langle N \rangle\,. \tag{41}$$

Result (41) can be obtained in a number of other ways, for example, by using the Keldysh diagram technique for non-equilibrium systems, and by analyzing the imaginary part of the self-energy function of bosons taking into account the in- and outflow of particles (a general approach to describing the nonequilibrium condensation of excitons and exciton polaritons within the framework of the Keldysh technique is developed in [117]), or by using the operator equations for ψ and $\psi^\dagger$ within the framework of the Langevin approach [118]. Thus, as the ground state is filled, the time of the condensate correlation increases, and the emission line of excitons is narrowed by analogy with the narrowing of the laser radiation line [110, 119, 120]. We note that, with an increase in the concentration of excitons, fluctuations in the number of particles (39) lead to a fluctuating shift of the exciton energy $\propto \mathcal{T}\delta n$ and, correspondingly, to a reduction in the correlation time [118]. In structures with microcavities at a sufficiently high pumping rate, in addition to the phase of the non-equilibrium condensate of exciton polaritons, a phase corresponding to lasing directly from the photon cavity mode is possible (the system transits to the weak coupling regime) [121]. A detailed review of nonlinear effects in microcavities under conditions of resonant excitation is given in Ref. [122].

The spatial correlations of excitons can be determined by linearizing Eqn (40). As an alternative, it is convenient to use the hydrodynamic approach, describing interacting excitons as an ideal liquid [4, 29, 40, 100]. We will focus on the case of zero temperature, when thermal fluctuations can be ignored. Correspondingly, small fluctuations of the particle concentration, δn, and the velocity $\mathbf{v}$ (in a stationary situation $\mathbf{v} \equiv 0$, $N \equiv N(\mathbf{r})$) satisfy the system of equations [4, 29, 40, 100, 123]

$$\frac{\partial \delta n}{\partial t} + \nabla (N\mathbf{v}) + \frac{\delta n}{\tau_N} = \delta g\,, \tag{42a}$$

$$\frac{\partial \mathbf{v}}{\partial t} + \frac{1}{m}\,\nabla \delta p = 0\,, \tag{42b}$$

where the pressure fluctuation $\delta p = \mathcal{T}\delta n$, and $\delta g \equiv \delta g(\mathbf{r}, t)$ is the fluctuation of the exciton generation rate, which maintain the rms fluctuation of the number of particles $\langle \delta n^2 \rangle$, Eqn (39).[7] In the linearized equation (42a), we disregarded the dependence of the stationary density on the coordinates. Taking into account the fluctuation potential in this approach is reduced to replacing $N \to N(\mathbf{r})$ in Eqn (42a), while the relationship between the fluctuations of pressure and concentration δp and δn in (42b) remains the same.

To analyze the role of the finite exciton lifetime in Eqn (42a), the dependence of the average concentration of particles N on coordinates and scattering amplitude $\mathcal{T}$ on energy can be disregarded. Writing

$$\mathbf{v}(\mathbf{r}) = \frac{1}{m}\,\nabla\varphi(\mathbf{r})$$

and performing the Fourier transform in the coordinates and time for fluctuations of the phase $\varphi \propto \varphi_{\mathbf{k},\omega} \exp(-\mathrm{i}\omega t + \mathrm{i}\mathbf{kr})$, we have

$$-\mathrm{i}\omega\left(-\mathrm{i}\omega + \frac{1}{\tau_N}\right)\varphi_{\mathbf{k},\omega} + \frac{\mathcal{T}N}{m}\,k^2\varphi_{\mathbf{k},\omega} = -\mathcal{T}g_{\mathbf{k},\omega}\,. \tag{43}$$

Hence, putting the Fourier components of the pump fluctuations $g_{\mathbf{k},\omega} = 0$, we see that the spectrum of elementary excitations — phonons in the exciton condensate — according to [29, 111, 112] is described by the relation

$$\omega\left(\omega + \frac{\mathrm{i}}{\tau_N}\right) = \frac{\mathcal{T}N}{m}\,k^2\,, \tag{44}$$

and in the low-frequency region it is diffusive:

$$\omega \approx -\mathrm{i}Dk^2\,, \tag{45}$$

where the effective diffusion coefficient is $D = \mathcal{T}N\tau_N/m$. For sufficiently large k, the frequency acquires the real part sk, where

$$s = \sqrt{\frac{\mathcal{T}N}{m}} \tag{46}$$

is the velocity of sound (cf. with (9) and (11)). The dispersion of elementary excitations is shown in Fig. 11. It can be seen from the plots that the spectrum does not satisfy the Landau superfluidity criterion. This is natural, since in the open system of excitons there is energy dissipation due to the competition between the processes of excitons entering and leaving the condensate. On the other hand, as the analysis performed in Ref. [29] shows, small spatially concentrated perturbations in such a system propagate with the velocity of sound.

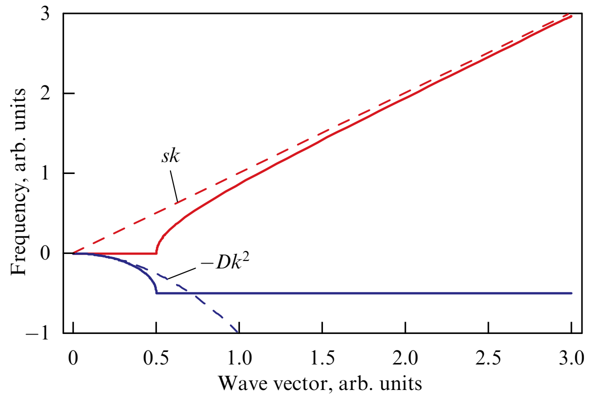

Figure 11. Spectrum of elementary excitations in a nonequilibrium exciton condensate. The solid curves show the real and imaginary parts of the frequency ω found from Eqn (44), the dashed curves show the real and imaginary parts found using asymptotic formulas (46) and (45). (From [29].)

Equations (42) also make it possible to calculate the correlator of the condensate phases,

$$\Phi(\mathbf{r}, t) = \left\langle \varphi(\mathbf{r} + \mathbf{r}', t + t')\varphi(\mathbf{r}', t')\right\rangle,$$

and, finally, a single-particle density matrix (ignoring fluctuations of the condensate population N),

$$\rho(\mathbf{r}_1, \mathbf{r}_2) = N\exp\left[-\frac{\Phi(\mathbf{r}_1 - \mathbf{r}_2, 0)}{2}\right]. \tag{47}$$

The calculation shows that, up to a common factor in a two-dimensional system [29],

$$\Phi(\mathbf{r}, t) \propto -\ln\left(\frac{Dt}{r^2}\right). \tag{48}$$

Thus, the phase correlation function behaves like $\ln(Dt/r^2)$, which means that the condensate density matrix (47) at large distances decreases according to a power law. Note that for $t \to 0$ the factor Dt should be replaced with k_m^{-2}, where the wave vector $k_m \sim ms$ is determined from the condition for the transition of the dispersion of elementary excitations from linear to quadratic [29]. A comparison of Eqn (48) and the corresponding expressions in Refs [4, 70, 124, 125] shows that Eqn (48) is applicable to the equilibrium situation with the corresponding replacement of the prefactor with a value proportional to the temperature T. Thus, in a two-dimensional system, the pump fluctuations, along with the effects of finite temperature, destroy the long-range order in the condensate of excitons. Nevertheless, at not too high temperatures $T \lesssim T_{\mathrm{2D}}$, the single-particle density matrix decreases with distance according to a power law:

$$\rho(\mathbf{r}_1, \mathbf{r}_2) \propto |\mathbf{r}_1 - \mathbf{r}_2|^{-\eta}\,, \tag{49}$$

where the exponent

$$\eta = \begin{cases} \dfrac{m\mathcal{T}}{32\pi} = \dfrac{1}{16\ln\left(mE_0/(2\pi N)\right)}\,, & \text{pump fluctuations} \\[2ex] \dfrac{mT}{2\pi N_{\mathrm{s}}}\,, & \text{thermal fluctuations} \end{cases} \tag{50}$$

---

[7] The correlator of the Fourier components of the lasing fluctuations has the form $\langle g_{\mathbf{k},\omega}\, g_{\mathbf{k}',\omega'}\rangle = g_0\delta_{\mathbf{k},-\mathbf{k}'}\delta(\omega + \omega')$, where $g_0 = 4\pi\langle N\rangle\tau_N^{-1}$. In Ref. [29], in the system of equations similar to (42), no distinction was made between τ_0 and τ_N.

is determined by the magnitude of exciton interaction and temperature, and N_s is the concentration of the superfluid component. The second equality in the upper line is obtained taking into account expression (31). To numerical factors, the exponent is determined by the ratio of the characteristic energy of particle interaction $\mathcal{T} N$ (if the pump fluctuations dominate) or the temperature T (if thermal fluctuations dominate) to the degeneracy temperature of the gas $T_{2D} \sim N/m$. At relatively small exciton concentrations, the exponent η is determined by thermal fluctuations, and at sufficiently large concentrations by interaction. It is noteworthy that in this case η depends on the concentration only logarithmically. With an increase in the temperature for the fixed concentration of particles, the exponent η increases, and at a certain critical temperature (or concentration of particles), power law (49) should change to an exponential one. For equilibrium two-dimensional systems, this corresponds to the BKT transition [4].

For completeness, we present expressions for the single-particle density matrix of a two-dimensional system of noninteracting excitons without disorder. In this case, the simple relation ($r = |\mathbf{r}_1 - \mathbf{r}_2|$) holds [22, 126],

$$\rho(r) = \int_0^{\infty} f(E; T, \mu)\, J_0\big(\sqrt{2mE}\, r\big) \mathcal{D}_{2D}\, \mathrm{d}E\,,$$

where $J_0(x)$ is the Bessel function of the first kind; recall that $\mathcal{D}_{2D}$ is the density of states in a two-dimensional system. In the limiting cases of nondegenerate and degenerate excitons, we obtain

$$\rho(r) \propto \begin{cases} \exp\left[-(k_{\mathrm{T}} r)^2\right], & T \gg T_{2D}\,, \\ K_0(k_\mu r) \propto r^{-1/2} \exp(-k_\mu r)\,, & T \ll T_{2D}\,. \end{cases} \qquad (51)$$

Recall that T_{2D} is the degeneracy temperature of the two-dimensional exciton gas, $k_{\mathrm{T}} = \sqrt{mT/2}$ is the characteristic heat wave vector, and $k_\mu = \sqrt{2m|\mu|}$ is a characteristic wave vector determined by the chemical potential of excitons. Note that for a degenerate gas $k_\mu \ll k_{\mathrm{T}}$, and the correlation length of degenerate excitons is noticeably greater than the correlation length in a nondegenerate gas [22, 126]. The dependence $\rho(r)$ for nondegenerate and degenerate statistics of excitons, as well as for interacting particles, is shown in Fig. 12.

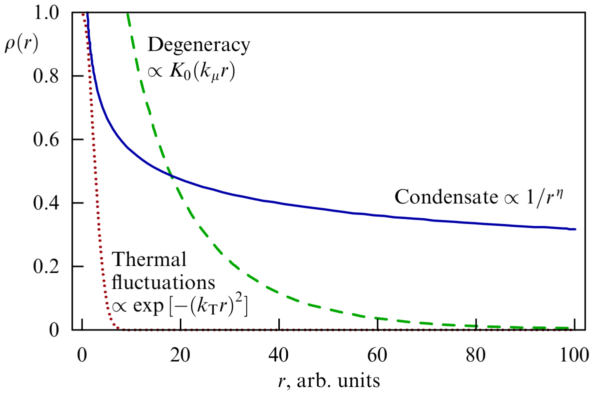

Figure 12. First-order correlation function $\rho(r)$ for a two-dimensional nondegenerate Bose gas (dotted curve), degenerate gas (dashed curve), calculated by Eqn (51), and for nonequilibrium condensate (49) (solid curve).

3.8 Manifestations of condensation of excitons in experiments

A number of papers have reported on the discovery of a condensate of excitons and exciton polaritons. The first experimental observations were as follows:

(1) Threshold appearance of an indirect exciton emission line (I-line) at a fixed pump power and a decrease in temperature below the critical value, or at a fixed temperature and an increase in the pump power [18].

(2) Spatial compression of the region from which the emission of spatially indirect excitons occurs with decreasing temperature [19].

(3) Threshold growth of intensity and narrowing of the photoluminescence line of exciton polaritons with increasing pump power [21].

However, the most convincing experimental evidence of the condensation of two-dimensional excitons and exciton polaritons is the observation of their first-order coherence (17). For this purpose, interference measurements were carried out (see, e.g., [20, 127]) for structures with spatially indirect excitons and [21] for exciton polaritons. Interference was observed between the points of the condensate, spaced apart at distances from several units to tens of micrometers [20, 22, 125, 127–130] (Fig. 13), which significantly exceeds the thermal wavelength of excitons. Note that with an increase in the number of particles, when the two-dimensional Bose gas becomes degenerate, but no condensate is formed, an increase in the length of spatial coherence may be associated with a decrease in the chemical potential of excitons or exciton polaritons (see (51) and Fig. 12), which somewhat complicates the interpretation of experiments [22, 126].

Reference [125] reported a power-law decay of the correlator (49) for exciton polaritons in a microcavity when the pump power exceeds the threshold value (cf. Fig. 13d and 13e); an analysis of the exponent η as a function of the pump power shows that the damping is determined precisely by the nonequilibrium nature of the exciton–polariton condensate. As shown in [22], nonequilibrium effects can play a significant role and increase the spatial coherence of excitons, even if the interaction between particles is insignificant.

We note that detailed studies of the distribution function of exciton polaritons were carried out in structures with microcavities [21, 131]. The possibility of controlling the detuning between the exciton and photon in one sample, and hence of changing the dispersion of exciton polaritons and their lifetimes and energy relaxation rates, allows observing a transition between strongly nonequilibrium and practically equilibrium situations [131]. The formation of vortices in an exciton–polariton condensate was also studied (see, e.g., [132]); superfluid propagation of the condensate was observed [133] (review in [134]), as was the emergence of solitons [135, 136]. However, some of the results obtained can be interpreted without involving the concepts of condensate and superfluidity [137].

Another experimental platform for the study of condensation is electron–hole excitations in the regime of the quantum Hall effect and like systems [138–141]. A discussion of such systems is beyond the scope of this review.

4. Other collective phases of excitons

The ideas of Bose–Einstein condensation of excitons discussed above were based on the simplest model, in which the interaction between excitons was considered to be short-

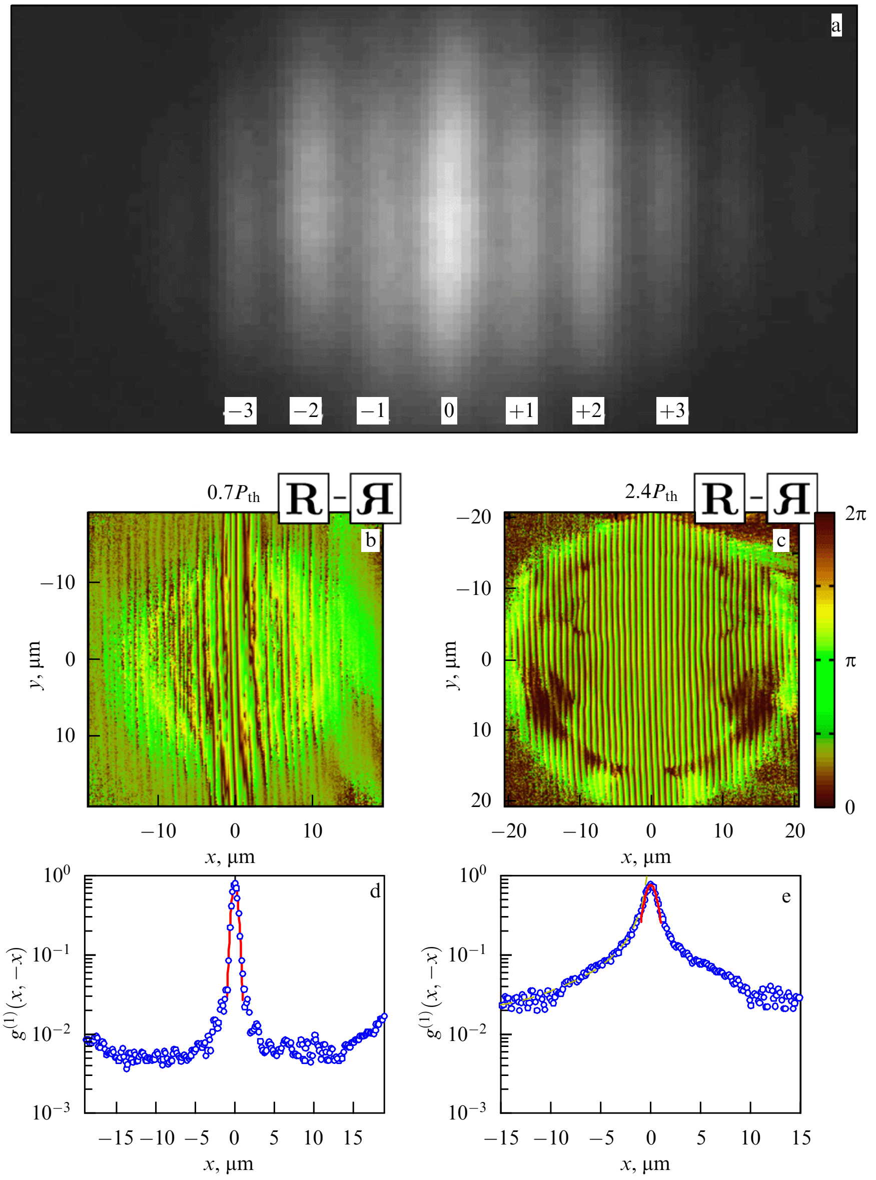

Figure 13. (a) Light interference pattern from a pair of spots spaced 5 μm apart in an opaque Schottky gate above a GaAs/AlGaAs quantum well 250 Å wide. (From [20].) (b, c) Interference maps of the emission of exciton polaritons in a microcavity in GaAs, placed in a Michelson interferometer below (b) and above (c) the condensation threshold. (d, e) Dependence of the first-order coherence on the distance at the same pump powers as in Fig. b, c. The curves represent a fitting within the model developed in [125]. ((b–e) From [125].)

range, and the exciton–exciton scattering amplitude $\mathcal{T} > 0$, which corresponds to the repulsion between particles. Generally, this is not the case. In particular, in structures with spatial separation of charge carriers, the interaction between excitons is determined by the relatively long-range $\propto 1/r^3$ dipole–dipole repulsion of particles. Furthermore, as is well known, excitons can bind like atoms to form excitonic molecules — biexcitons [142]. Even if the spin configuration of the excitons prevents the formation of bound pairs, the van der Waals attraction of excitons is possible at large distances between particles. All this offers a possibility of implementing various collective phases of excitons. Let us briefly describe some of them, which in our opinion are the most realistic.

4.1 Bose systems with short-range repulsion and long-range attraction

Consider spatially direct excitons within the framework of a hydrogen-like model. As for two neutral atoms, the effective potential energy of interaction between excitons can be approximately divided into two contributions. The 'short-range' contribution, which is manifested at small distances between the excitons $r \lesssim a_B$ (recall that a_B is the Bohr radius of the exciton), is mainly due to the exchange interaction between identical charge carriers making up the exciton [93, 143, 144]. The 'long-range' contribution manifests itself at $r \gg a_B$; it is mainly due to polarization or van der Waals interaction between excitons [145, 146]. For excitons in the ground state, the van der Waals interaction has the character of attraction, since the fluctuation of the dipole moment in one of the excitons induces the dipole moment in the other exciton in such a way that the total energy of the pair decreases [92]. Therefore, attraction is possible at large distances between spatially direct excitons. Note that the situation changes dramatically for spatially indirect excitons in structures with single or double quantum wells, where dipole–dipole repulsion of excitons dominates at large distances (see Section 4.2). The sign of a short-range contribution to the potential energy of exciton–exciton interaction is usually positive, which corresponds to repulsion between particles.

Collective phenomena in a system of bosons with short-range repulsion and long-range attraction were discussed in [147, 148] for a three-dimensional system. Here, we give a simple consideration using the self-consistent field approximation. We represent the potential energy of interaction in the form

$$V(r) = V_{\mathrm{core}}(r) - U(r)\,,$$

where $V_{\mathrm{core}}(r) > 0$ is the short-range repulsive part and $-U(r)$ is the long-range contribution corresponding to attraction. As above, the short-range part will be characterized by the scattering amplitude f, and the long-range part by the effective power $U_0 = \int U(r)\,\mathrm{d}\mathbf{r}$. Let us describe the energy spectrum of such a system in the low-density approximation with respect to the short-range part of the potential, $Nf^{\,\mathrm{D}} \ll 1$ (D being the dimension of the system), and in the self-consistent field approximation with respect to the long-range part. First, consider excitons in a bulk semiconductor. At zero temperature, the energy of the ground state of the system, per unit volume, can be written in the form[8] (only pair interactions are taken into account [4, 149])

$$\varepsilon = \frac{2\pi f}{m}\,N^2\left(1 + \gamma_3\sqrt{Nf^{\,3}}\,\right) - \frac{1}{2}\,N^2 U_0\,, \tag{52}$$

where the numerical coefficient is $\gamma_3 = 128/(15\sqrt{\pi})$, and the dimensionless parameter $\sqrt{Nf^{\,3}}$ is considered small. Depending on the concentration of particles, the energy density ε has a minimum at

$$N = N_{\mathrm{cr}} \equiv \left[\frac{4}{5\gamma_3 f^{3/2}}\left(\frac{mU_0}{4\pi f} - 1\right)\right]^2, \quad U_0 > U_{\mathrm{cr}} = \frac{4\pi f}{m}\,. \tag{53}$$

Indeed, when the condition $U_0 > U_{\mathrm{cr}}$ is satisfied at a low concentration of particles, the long-range attraction dominates, and the energy of the excitonic gas decreases with increasing concentration. When $N > N_{\mathrm{cr}}$, the short-range repulsion begins to act, and $\varepsilon(N)$ begins to increase due to the term $\propto \gamma_3$. If $U_0 < U_{\mathrm{cr}}$, then $\varepsilon(N)$ increases monotonically with growing concentration, because the long-range contribution is less than the short-range one.

To determine the stability conditions for the system excitation spectrum, it is sufficient to determine the compressibility of an imperfect Bose gas. Writing down the total energy of the gas $E = \varepsilon\mathcal{V}$ depending on the total number of bosons $N\mathcal{V}$, where $\mathcal{V}$ is the volume of the system, we have for the pressure p and the sound velocity s [4]

$$p = -\frac{\partial E}{\partial \mathcal{V}} = N^2\left[\frac{2\pi f}{m}\left(1 + \frac{3}{2}\,\gamma_3\sqrt{f^3 N}\right) - \frac{U_0}{2}\right], \tag{54a}$$

$$s = \sqrt{\frac{1}{m}\frac{\partial p}{\partial N}} = \left(\frac{N}{m}\right)^{1/2}\left[\frac{4\pi f}{m}\left(1 + \frac{15}{8}\,\gamma_3\sqrt{f^{\,3}N}\right) - U_0\right]^{1/2}, \tag{54b}$$

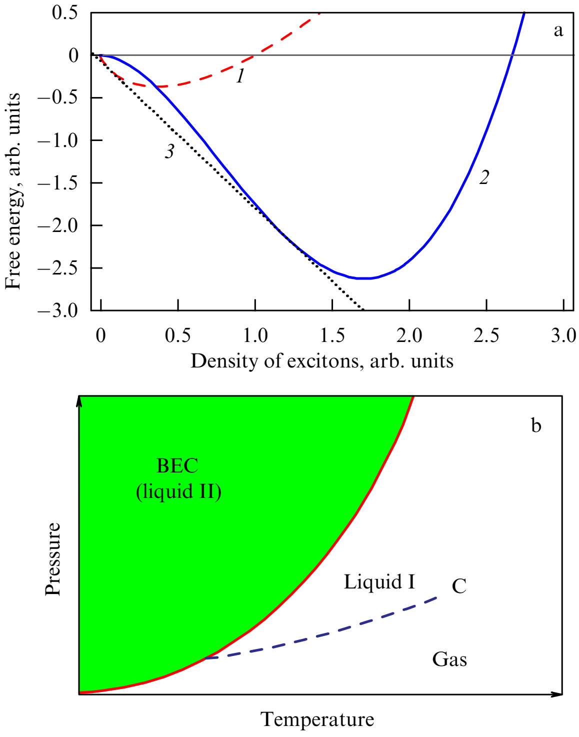

Figure 14. (a) Free energy of an ideal gas of excitons (red dashed curve *1*) and free energy of condensate (52) (blue solid curve *2*), as well as their mutual tangent *3*. It is assumed that $U_0 > U_{\mathrm{cr}}$. (b) Phase diagram in the temperature–pressure axes from [147]. The solid red curve shows the transition to the state of Bose–Einstein condensate (BEC or liquid II, with the interparticle interaction taken into account). The dashed curve shows a transition of the first kind from gas to classical liquid (liquid I), C is the critical point.

in accordance with [148]. Naturally, at $U_0 = 0$ in the low-density approximation, the formula for the velocity of sound (see Eqn (59) below) transforms into the well-known expression (11). Note that for $N \geqslant N_{\mathrm{cr}}$, the pressure is positive, and the velocity of sound is real, i.e., the system is thermodynamically stable. Correspondingly, for a Bose gas with long-range attraction and short-range repulsion, the spectrum of elementary excitations has an acoustic character, and the system (for $N \geqslant N_{\mathrm{cr}}$) behaves like a condensate.

When $N < N_{\mathrm{cr}}$, the system breaks up into droplets of condensate, between which there is a strongly rarefied exciton gas. The phase equilibrium between condensate droplets and a gas is illustrated in Fig. 14a: in the simplest model, a rarefied gas of excitons is described by the free energy density

$$\mathcal{F}_{\mathrm{id}} = -NT\,\ln\left(\frac{N_{\mathrm{d}}}{N}\right), \tag{55}$$

where N is the concentration of excitons, N_{d} is the concentration of the exciton gas degeneracy, T is the temperature, and for the condensate one can use the approximation of zero temperature and Eqn (52), $\mathcal{F}_{\mathrm{cond}} = \varepsilon$. The phase equilibrium condition requires equality of chemical potentials and pressures, i.e., the existence of a common tangent to the curves shown in Fig. 14a. The phase diagram of states of such a system, found in Ref. [147] and shown in Fig. 14b, turns out to be very rich. In addition to the condensate (BEC or liquid II by analogy with liquid helium physics) and the gas state, there is a state of a normal liquid (liquid I); between this liquid and

---

[8] Strictly speaking, with the screening of the exciton–exciton interaction taken into account [41, 98], the power of the potential U_0 in this expression should be replaced by $\tilde{U}_0 = N^{-2}\int U(r)\mathcal{K}_2(r)\,\mathrm{d}\mathbf{r}$, where $\mathcal{K}_2(r)$ is the pair correlation function of bosons.

the gas there is a phase transition of the first kind (dashed curve). As in the classical theory of phase transitions, the transition between the gas phase and liquid I is possible only at temperatures that do not exceed the temperature of the critical point. The difference between liquids I and II is that in liquid II the ground state of the system turns out to be macroscopically populated.

We emphasize that the issue of the state diagram for a system of bosons capable of forming a Bose–Einstein condensate and attracting at large interparticle distances is rather nontrivial. Two scenarios are possible here. The first one is realized with a rather weak attraction between bosons and small values of their masses. In this case, as the temperature decreases, Bose–Einstein condensation occurs in the gas phase, and only then does a phase transition from the gas phase to the liquid occur. The second scenario takes place for a sufficiently strong attraction of particles and/or large values of their masses. Under these conditions, when the temperature is lowered, the gas–liquid phase transition first occurs, and the macroscopic population of the ground energy level with bosons occurs already in the liquid phase. In this case, due to the interaction, the fraction of particles in the Bose–Einstein condensate is small. Such a scenario (gas–liquid transition followed by Bose condensation), apparently, is realized in helium, where the fraction of condensate is about 7%.

Let us roughly estimate the relations between the parameters separating these scenarios. In order to realize the first scenario, the temperature of the Bose–Einstein condensation $T_c \sim N^{2/3}/m$ (Eqn (6)) should exceed the critical temperature T_{cr} of the transition in the gas–liquid system at the critical concentration $N = N_{cr}$. These parameters can be estimated in the order of magnitude within the framework of the van der Waals model [3]:

$$T_{cr} \sim \frac{1}{a^3}\int U(r) r^2 \, dr \sim \frac{U_0}{a^3}\,, \quad N_{cr} \sim \frac{1}{a^3}\,, \tag{56}$$

where a is the effective radius of the (short-range) potential of interparticle repulsion; recall that U_0 is the power of the attracting part of the potential. As a result, in the three-dimensional case, we obtain

$$\begin{cases} \dfrac{a}{m} \gg U_0 \;\Rightarrow\; \text{Bose condensation first,} \\ \dfrac{a}{m} \ll U_0 \;\Rightarrow\; \text{gas}-\text{liquid transition first.} \end{cases}$$

It is important to note that the radius of action of the repulsive part of the potential a and the scattering amplitude f in (52) are of the same order. Within the framework of the above considerations, the minimum of the dependence of the condensate energy $\varepsilon(N)$ and the possibility of droplet formation arise only when $U_0 > U_{cr}$ (see Eqn (53)). Thus, the described model is adequate only for a sufficiently strong attraction, i.e., it corresponds to the second scenario: gas–liquid transition followed by condensation.

In a two-dimensional system, the energy of a Bose gas per unit volume can be written as

$$\varepsilon = \frac{2\pi N^2}{m}\,\frac{1}{\ln\left[\gamma_2/(Na^2)\right]} - \frac{1}{2}\,N^2 U_0\,. \tag{57}$$

Here, γ_2 is a parameter of the order of unity, and the quantity $U_0 = \int U(r)\,d\mathbf{r}$, as above, describes the long-range attraction in the mean field approximation. We emphasize that the average density approximation is fulfilled under the condition that $N \gg 1/a_{\text{long}}^2$, where a_{long} is the radius of action of the long-range part of the potential. The first term explicitly takes into account the logarithmic dependence of the scattering amplitude in a two-dimensional system; it is assumed that the logarithm in the denominator is large (cf. Eqn (31)). The calculation of contributions of the higher orders in Na^2 (as well as determination of γ_2) is extremely nontrivial. However, their analysis is beyond the scope of this review [75, 150–156]. The minimum in the dependence $\varepsilon(N)$ is attained when

$$N = N_{cr} \equiv \frac{\gamma_2}{a^2}\exp\left(-\frac{4\pi}{mU_0}\right), \tag{58}$$

with repulsion dominating for $N > N_{cr}$ and attraction for $N < N_{cr}$. Expression (58) is valid with exponential accuracy. In the same approximation, the velocity of sound can be written in the form

$$s = \sqrt{\frac{N}{m}\left(\frac{4\pi}{m}\,\frac{1}{\ln\left[\gamma_2/(Na^2)\right]} - U_0\right)}\,. \tag{59}$$

For $N > N_{cr}$, the velocity of sound $s > 0$, and the system is stable. A detailed analysis of the behavior of the system at $N = N_{cr}$ requires going beyond the approximation $\ln\left[\gamma_2/(Na^2)\right] \gg 1$ and is an interesting problem for further research.

Note, however, that the described model and the phase diagram proposed in [147] have limited applicability to real systems: in bulk semiconductors, as a rule, an electron–hole liquid is formed (see Section 4.3), and in the two-dimensional case, the formation of a crystal exciton phase is possible, which we will discuss in Section 4.2.

4.2 Gas–crystal phase transition

Let us consider spatially indirect (dipolar) excitons in the quasi-two-dimensional systems schematically shown in Fig. 3a, b. The interaction between these excitons can be described by the simple law

$$V(r) = \frac{2e^2}{\varkappa}\left(\frac{1}{r} - \frac{1}{\sqrt{r^2 + h^2}}\right) \approx \frac{e^2 h^2}{\varkappa r^3}\,. \tag{60}$$

Here, r is the distance between excitons in the structure plane, h is the characteristic distance between an electron and a hole along the normal to the plane of the wells, eh is the component of the exciton dipole moment normal to the plane of the wells, and $\varkappa$ is the permittivity of the medium. Expression (60) is valid for $h \gg a_B$ (a_B is the Bohr radius of an exciton), and, for $r \gg h$, the potential energy slowly, as $\propto r^{-3}$, decays with an increase in the distance between particles (see the approximate equality in Eqn (60)). In Ref. [36], it was predicted that, in addition to Bose–Einstein condensation, dipolar excitons at temperatures exceeding the expected condensation temperatures could form a crystal structure or, more precisely, a structure close to crystalline (with well-known reservations about the instability of two-dimensional crystals [3]). Below, for brevity, we will call this phase a crystal.

The possibility of crystallization of excitons with long-range repulsion (60) can be easily verified by analyzing the free energy of a weakly nonideal excitonic gas and the crystal.

For the gas phase, the free energy density has the form

$$\mathcal{F}_{\mathrm{gas}} = \mathcal{F}_{\mathrm{id}} + E_{\mathrm{C}}\,, \quad E_{\mathrm{C}} = \frac{1}{2}\int V(r)\,\mathcal{K}_2(r)\,\mathrm{d}\mathbf{r}\,, \tag{61}$$

where the free energy of a unit volume of the ideal gas is given by Eqn (57), the second term describes the contribution of Coulomb repulsion, and $\mathcal{K}_2(r)$ is the pair correlation function, which in the quasi-classical approximation[9] can be represented as

$$\mathcal{K}_2(r) = N^2 \exp\left(-\frac{V(r)}{T}\right). \tag{62}$$

Under conditions when the exciton gas is not degenerate, but the interaction is strong enough, $T \ll e^2/(\varkappa h)$, the Coulomb contribution is strongly suppressed, since a circle of radius $r_{\mathrm{T}} = [e^2 h^2/(\varkappa T)]^{1/3}$ near the exciton turns out to be inaccessible to other particles. As a result,

$$\mathcal{F}_{\mathrm{gas}} = -NT\ln\left(\frac{N_{\mathrm{d}}}{N}\right) + \frac{\pi\Gamma(4/3)}{h^2}\left(\frac{\varkappa hT}{e^2}\right)^{1/3}\frac{e^2}{\varkappa h}\,(Nh^2)^2\,, \tag{63}$$

where $\Gamma(x)$ is the gamma function.

For the crystal phase, the main contribution to the free energy density is made by the Coulomb repulsion of excitons located in the lattice sites. The calculation for a perfect triangular lattice performed in Ref. [36] yields

$$\mathcal{F}_{\mathrm{cryst}} \approx \frac{2.48}{h^2}\,\frac{e^2}{\varkappa h}\,(Nh^2)^{5/2} - NT\,\ln\left(\frac{g^g}{(g-1)^{g-1}}\right), \tag{64}$$

where the second term describes the entropy contribution, caused by the presence of spin degeneracy in excitons, and g is the degeneracy multiplicity.

A comparison of expressions (63) and (64) shows that at low temperatures the ordered distribution of excitons in space turns out to be energetically more favorable, since for $Nh^2 \ll 1$ the repulsion of excitons in the crystal phase turns out to be smaller due to the smallness of Nh^2. The phase equilibrium between the crystal and the gas can be analyzed using the same considerations as in Section 4.1 (Fig. 15a), where the free energies of the gas and crystal phases and their common tangent are presented. The phase diagram of the system of dipolar excitons, calculated in [36], is shown in Fig. 15b. The same diagram shows the concentration dependence of the temperature below which the exciton gas becomes degenerate (BEC region). Naturally, phonons in a two-dimensional crystal of excitons lead to the destruction of long-range order [3, 36]; therefore, an exciton crystal can also be called a liquid with a pronounced short-range order. In this case, the density correlation function $\langle n(\mathbf{r})n(\mathbf{r}+\mathbf{R})\rangle$, where $\mathbf{R}$ is the distance between the lattice nodes, due to lattice vibrations, falls off according to the power law $R^{-\alpha}$ [36]. The estimate made in Ref. [36] demonstrates that the exponent α is small.

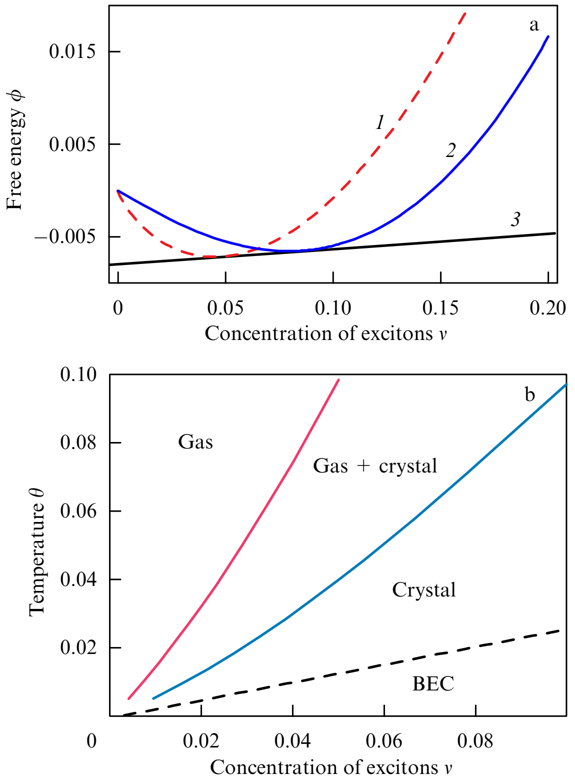

Figure 15. (a) Free energy density in dimensionless units $\phi = \mathcal{F}h^2/(e^2/\varkappa h)$ depending on the dimensionless concentration $\nu = Nh^2$. Red dashed curve *1* is the free energy of gas (63), solid blue curve *2* is that of crystal (64). Black curve *3* is their mutual tangent. The spin degeneracy factor is $g = 2$, $N_{\mathrm{d}}\,h^2 = 0.4$. (b) Phase diagram of a system of spatially indirect excitons. Dimensionless temperature $\theta = T/(e^2/\varkappa h)$. BEC denotes the region of parameters where the exciton gas becomes degenerate. (From [36].)

In Ref. [36], manifestations of an excitonic crystal in photoluminescence spectra were also analyzed. Using Eqns (63) and (64), it is possible to express the energy of interaction of excitons in the gas and crystal phases, which behave differently: $\mathcal{E}_{\mathrm{gas}}(N) \propto T^{1/3}N$ in the gas phase and $\mathcal{E}_{\mathrm{cryst}}(N) \propto N^{3/2}$ in the crystal phase. The value of the Coulomb energy determines the shift of the luminescence line as a function of particle concentration. At a fixed temperature and low concentrations of excitons, the center frequency of the exciton luminescence line increases linearly with increasing concentration. Then, upon reaching the boundary of the two-phase region, a luminescence line from the crystalline phase appears, and its intensity grows with a simultaneous decrease in the intensity of the gas phase line, the positions of the lines remaining unchanged. With a further increase in the concentration, the system leaves the two-phase region; only one line remains, the frequency shift of which is described by energy $\mathcal{E}_{\mathrm{cryst}}(N)$. This is illustrated in Fig. 16. Figures 16a and 16b differ in the values of the dimensionless temperature θ: the higher the temperature, the greater the energy of the Coulomb repulsion of excitons in the gas phase (the second term in Eqn (63)), in contrast to the repulsive energy in the crystal, where it does not depend on temperature (see the first term in Eqn (64)). Therefore, in the two-phase region, the Coulomb frequency shift in the gas phase at a high temperature is greater than that in a crystal, while at a low temperature it is vice versa.

Stern and Bar-Joseph experimentally discovered the occurrence of two phases in a two-dimensional system of dipolar excitons; a description of the obtained results is given in Refs [77, 159]. An important open question is the self-consistent model description of such a system.

---

[9] Describing two-dimensional systems with dipole–dipole repulsion in the classical case is a separate problem (see, e.g., [157, 158] and references therein).

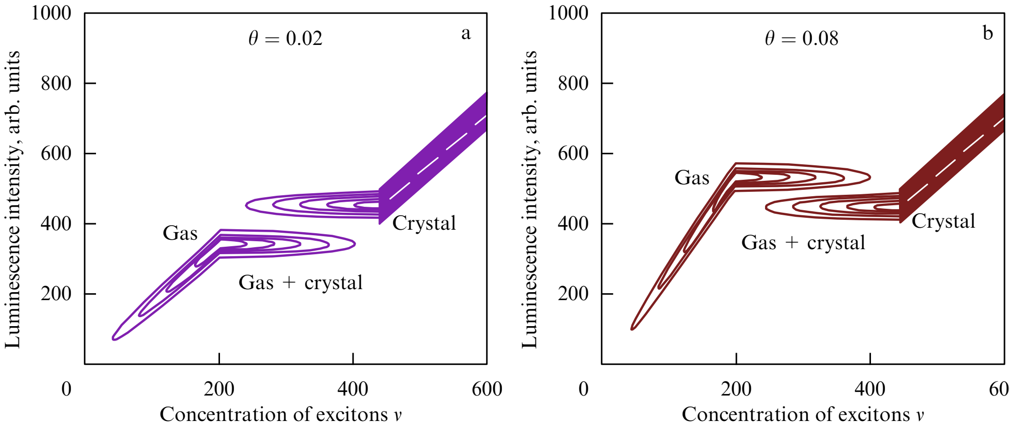

Figure 16. Change in the luminescence spectrum versus dimensionless concentration $\nu = Nh^2$ for two different dimensionless temperatures $\theta = T/(e^2/\varkappa h)$: (a) $\theta = 0.02$, (b) $\theta = 0.08$. Lines of equal luminescence intensity are schematically shown. (From [36].)

4.3 Electron–hole liquid

For Wannier–Mott excitons in most typical semiconductors, the masses of an electron m_e and a hole m_h are rather close, and the adiabaticity parameter $(m_e/m_h)^{1/4}$ is not small. In a bulk semiconductor or structures with quantum wells, where spatially direct (rather than dipolar) excitons are realized, the formation of an exciton crystal is impossible. Indeed, from general considerations [3, 34] it is known that the crystal phase should arise at the critical exciton concentration $N_c \sim a_B^{-D}$ (a_B is the Bohr radius of the exciton, D = 2 or 3 is the dimension of the system). But then the amplitude of zero-point oscillations of excitons would be of the order of a_B, which would lead to the melting of the crystal.[10] Based on these considerations, Keldysh in 1968 predicted the possibility of the formation of an electron–hole liquid, i.e., a degenerate two-component liquid of electrons and holes [31]. In fact, the behavior of electrons and holes in such a liquid is analogous to the behavior of a collective of electrons in a metal: the particles turn out to be delocalized and can propagate freely and independently over the volume of the liquid, naturally, without violating the electrical neutrality of the system. An electron–hole liquid was first observed by Pokrovskii and Svistunova in Ge crystals [160].

A large number of reviews [31–34], including modern papers [35, 161], have been devoted to the physics of electron–hole liquids in semiconductors and semiconductor nanostructures; therefore, we will very briefly list the main features of such a phase. The critical temperature and the concentration of exciton condensation into an electron–hole liquid can be estimated for a bulk semiconductor as [34]

$$T_c \sim 0.1 E_B\,, \quad N_c \sim \frac{1}{a_B^3}\,, \qquad (65)$$

where E_B is the exciton binding energy. The phase diagram of the electron–hole liquid is shown schematically in Fig. 17. In the region of parameters of gas and liquid coexistence, the system breaks up into droplets of liquid phase surrounded by a gas of excitons (compare with the scenarios considered in Sections 4.1 and 4.2).

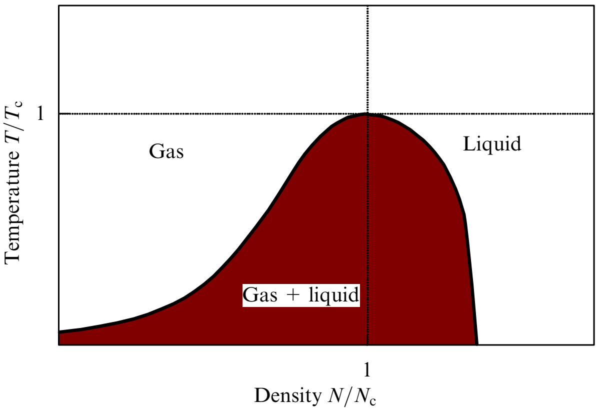

Figure 17. Schematic phase diagram of an electron–hole liquid. (From [34].)

The energy of particles in a liquid consists of the Fermi energies of electrons and holes, as well as the potential energy of their Coulomb interaction. Due to Coulomb correlations in an electron–hole liquid, the energy of the liquid decreases in comparison with the energy of noninteracting particles, and the luminescence line of the liquid turns out to be below the absorption edge of a nonexcited semiconductor. In multivalley Si and Ge crystals, exciton recombination is possible only with the participation of phonons, and the photoluminescence spectrum of an electron–hole liquid acquires the characteristic 'triangular' shape.

5. Conclusion

In this review, we outline the main points in the development of the concept of collective effects in exciton systems.

In bulk semiconductors, as well as in atomic systems, the formation of a Bose–Einstein condensate of excitons is possible. Due to the interaction between excitons, the condensate will be superfluid, and a weak random potential does not significantly affect its properties. The formation of a condensate state can manifest itself in the optical response of a semiconductor in the form of two spectral lines, corresponding to amplification and absorption of radiation, separated by twice the energy of a condensate phonon with a wave vector equal to the wave vector of light at the frequency of exciton resonance.

---

[10] Note that for dipolar or spatially indirect excitons the situation is richer; one more parameter, $h \gg a_B$ (the distance between the layers), appears in the system, and the short-range order of the exciton arrangement may be explicitly expressed, as discussed in Section 4.2.

The situation turns out to be radically different in two-dimensional systems. From the general theory for ideal systems, it follows that, at a finite temperature, the phase transition to the condensate state is impossible, but a system of two-dimensional bosons at low temperatures can possess superfluidity [4]. Real systems in which the collective behavior of two-dimensional or quasi-two-dimensional excitons is investigated, namely, structures with single and double quantum wells, as well as with microcavities, possess a disorder, which makes the picture of collective effects very rich. Thus, in contrast to the ideal two-dimensional system, in a system with disorder, the Bose–Einstein condensation of excitons is possible. The repulsion between particles leads to a limitation of the number of excitons in potential wells and screening of the fluctuation potential, due to which the system can transit to a superfluid state. An additional specificity is introduced by the finite lifetime of excitons. First, it leads to a seemingly paradoxical result: the existence of a low-temperature boundary of the condensation region in the phase diagram of excitons. Second, due to a finite lifetime, excitons can exist only in the presence of pumping, whose fluctuations, along with thermal fluctuations, destroy long-range order.

The review also briefly analyzes the gas–crystal transition in a system of dipolar excitons, and provides basic information about the electron–hole liquid in semiconductors.

Despite the fact that during almost sixty years of investigating collective effects in exciton systems in semiconductors the main aspects of exciton condensation have become understood, both theoretical and experimental studies in this area are far from complete. In theory, important tasks are to construct the phase diagram of excitons for realistic systems and to refine the boundaries of the regions of condensation and crystallization of excitons, the transition of an excitonic liquid to the superfluid state, and to study the possibilities of the coexistence of a condensate and an electron–hole liquid. A relevant problem is the implementation of the crossover between the exciton condensate and the condensate of fermion pairs [162] by analogy with the crossover between the superconducting states (BCS — Bardeen–Cooper–Schrieffer theory) and condensate states of atoms (BCS–BEC) [163, 164]. The emergence of new material systems, in particular, semiconductors based on atom-thin crystals that demonstrate unusually strong exciton effects [165, 166], poses new problems for both experiment and the theory of exciton condensates. Such studies are now at their initial stages [54, 55, 167, 168].

References

1. Bose S *Z. Phys.* **26** 178 (1924)
2. Einstein A *Sitzungsber. Preuß. Akad. Wiss. Phys.-Math. Kl.* (1) 3 (1925)
3. Landau L D, Lifshitz E M *Statistical Physics* Vol. 1 (London: Butterwoth-Heinemann, 2008); Translated from Russian: *Statisticheskaya Fizika* Pt. 1 (Moscow: Nauka, 1976)
4. Lifshitz E M, Pitaevskii L M *Statistical Physics* Vol. 2 (Oxford: Pergamon Press, 1980); Translated from Russian: *Statisticheskaya Fizika* Pt. 2 (Moscow: Fizmatlit, 2001)
5. Lifshitz I M *Sov. Phys. JETP* **11** 1130 (1960); *Zh. Eksp. Teor. Fiz.* **38** 1569 (1960)
6. Blanter Ya M et al. *Phys. Rep.* **245** 159 (1994)
7. Anderson M H et al. *Science* **269** 198 (1995)
8. Davis K B et al. *Phys. Rev. Lett.* **75** 3969 (1995)
9. Bogolyubov N N *Izv. Akad. Nauk SSSR Ser. Fiz.* **11** 77 (1947); *Usp. Fiz. Nauk* **93** 552 (1967); Bogolubov N *J. Phys. USSR* **11** 23 (1947)
10. Rashba E I, Sturge M D (Eds) *Excitons* (Modern Problems in Condensed Matter Sciences, Vol. 2) (Amsterdam: North-Holland Publ. Co., 1982)
11. Klingshirn C F (Ed.) *Semiconductor Optics* (New York: Springer, 2012)
12. Moskalenko S A *Sov. Phys. Solid State* **4** 199 (1962); *Fiz. Tverd. Tela* **4** 276 (1962)
13. Blatt J M, Böer K W, Brandt W *Phys. Rev.* **126** 1691 (1962)
14. Keldysh L V, Kozlov A N *JETP Lett.* **5** 190 (1967); *Pis'ma Zh. Eksp. Teor. Fiz.* **5** 238 (1967)
15. Gergel' V A, Kazarinov R F, Suris R A *Sov. Phys. JETP* **26** 354 (1968); *Zh. Eksp. Teor. Fiz.* **53** 544 (1967)
16. Agranovich V M, Toshich B S *Sov. Phys. JETP* **26** 104 (1968); *Zh. Eksp. Teor. Fiz.* **53** 149 (1967)
17. Butov L V et al. *Phys. Rev. Lett.* **73** 304 (1994)
18. Larionov A V et al. *JETP Lett.* **75** 570 (2002); *Pis'ma Zh. Eksp. Teor. Fiz.* **75** 689 (2002)
19. Butov L V et al. *Nature* **417** 47 (2002)
20. Gorbunov A V, Timofeev V B *JETP Lett.* **84** 329 (2006); *Pis'ma Zh. Eksp. Teor. Fiz.* **84** 390 (2006)
21. Kasprzak J et al. *Nature* **443** 409 (2006)
22. Belykh V V et al. *Phys. Rev. Lett.* **110** 137402 (2013)
23. Shilo Y et al. *Nat. Commun.* **4** 2335 (2013)
24. Krauth W, Trivedi N, Ceperley D *Phys. Rev. Lett.* **67** 2307 (1991)
25. Falco G M, Nattermann T, Pokrovsky V L *Phys. Rev. B* **80** 104515 (2009)
26. Bertoli G et al. *Phys. Rev. Lett.* **121** 030403 (2018)
27. Aleiner I L, Altshuler B L, Shlyapnikov G V *Nat. Phys.* **6** 900 (2010)
28. Michal V P et al. *Proc. Natl. Acad. Sci. USA* **113** E4455 (2016)
29. Glazov M M, Suris R A *J. Exp. Theor. Phys.* **126** 833 (2018); *Zh. Eksp. Teor. Fiz.* **153** 1001 (2018)
30. Tikhodeev S G *Sov. Phys. JETP* **70** 380 (1990); *Zh. Eksp. Teor. Fiz.* **97** 681 (1990)
31. Keldysh L V, in *Trudy IX Mezhdunarodnoi Konf. po Fizike Poluprovodnikov, Moskva, 23–29 Iyulya 1968 g.* (Proc. of the IX Intern. Conf. on Semiconductor Physics, Moscow, 23–29 July, 1968) (Leningrad: Nauka, 1969)
32. Keldysh L V *Sov. Phys. Usp.* **13** 292 (1970); *Usp. Fiz. Nauk* **100** 514 (1970)
33. Tikhodeev S G *Sov. Phys. Usp.* **28** 1 (1985); *Usp. Fiz. Nauk* **145** 3 (1985)
34. Jeffries C D, Keldysh L V *Electron-Hole Droplets in Semiconductors* (Modern Problems in Condensed Matter Sciences, Vol. 6) (Amsterdam: North-Holland Publ. Co., 1983)
35. Sibeldin N N *Phys. Usp.* **60** 1147 (2017); *Usp. Fiz. Nauk* **187** 1236 (2017)
36. Suris R A *J. Exp. Theor. Phys.* **122** 602 (2016); *Zh. Eksp. Teor. Fiz.* **149** 695 (2016)
37. Gross E F, Karryev N A *Dokl. Akad. Nauk SSSR* **84** 261 (1952)
38. Keldysh L V, Kozlov A N *Sov. Phys. JETP* **27** 521 (1968); *Zh. Eksp. Teor. Fiz.* **54** 978 (1968)
39. Combescot M, Combescot R, Dubin F *Rep. Prog. Phys.* **80** 066501 (2017)
40. Gergel' V A, Kazarinov R F, Suris R A *Sov. Phys. JETP* **27** 159 (1968); *Zh. Eksp. Teor. Fiz.* **54** 298 (1968)
41. Gergel' V A, Kazarinov R F, Suris R A *Sov. Phys. JETP* **31** 367 (1970); *Zh. Eksp. Teor. Fiz.* **58** 686 (1970)
42. Gastev S V et al. *Sov. Phys. Solid State* **25** 1733 (1983); *Fiz. Tverd. Tela* **25** 3002 (1983)
43. Snoke D W, Wolfe J P, Mysyrowicz A *Phys. Rev. Lett.* **64** 2543 (1990)
44. Snoke D W, Wolfe J P, Mysyrowicz A *Phys. Rev. B* **41** 11171 (1990)
45. Yoshioka K, Chae E, Kuwata-Gonokami M *Nat. Commun.* **2** 328 (2011)
46. Fröhlich D, Bayer M *Phys. Solid State* **60** 1600 (2018); *Fiz. Tverd. Tela* **60** 1581 (2018)
47. Snoke D, Kavoulakis G M *Rep. Prog. Phys.* **77** 116501 (2014)
48. Moskalenko S A, Snoke D W *Bose–Einstein Condensation of Excitons and Biexcitons and Coherent Nonlinear Optics with Excitons* (Cambridge: Cambridge Univ. Press, 2000)
49. Fortin E, Fafard S, Mysyrowicz A *Phys. Rev. Lett.* **70** 3951 (1993)
50. Benson E, Fortin E, Mysyrowicz A *Solid State Commun.* **101** 313 (1997)

51. Kavoulakis G M, Baym G *Phys. Rev. B* **54** 16625 (1996)
52. Koplevich G A, Tikhodeev S G, Gippius N A *J. Exp. Theor. Phys.* **82** 1180 (1996); *Zh. Eksp. Teor. Fiz.* **109** 2189 (1996)
53. Tikhodeev S G, Kopelevich G A, Gippius N A *Phys. Status Solidi B* **206** 45 (1998)
54. Fogler M M, Butov L V, Novoselov K S *Nat. Commun.* **5** 4555 (2014)
55. Wang Z et al. *Nature* **574** 76 (2019)
56. Butov L V *J. Exp. Theor. Phys.* **122** 434 (2016); *Zh. Eksp. Teor. Fiz.* **149** 505 (2016)
57. Kavokin A et al. *Microcavities* (Ser. on Semiconductor Science and Technology, No. 16) (Oxford: Oxford Univ. Press, 2011)
58. Timofeev V, Sanvitto D (Eds) *Exciton Polaritons in Microcavities* (New York: Springer, 2012)
59. Sun Y et al. *Phys. Rev. Lett.* **118** 016602 (2017)
60. Klaers J et al. *Nature* **468** 545 (2010)
61. Mermin N D, Wagner H *Phys. Rev. Lett.* **17** 1133 (1966)
62. Hohenberg P C *Phys. Rev.* **158** 383 (1967)
63. Coleman S *Commun. Math. Phys.* **31** 259 (1973)
64. Penrose O, Onsager L *Phys. Rev.* **104** 576 (1956)
65. Bogolubov N N, Bogolubov N N (Jr.) *Introduction to Quantum Statistical Mechanics* (Hackensack, NJ: World Scientific, 2010); Translated from Russian: *Vvedenie v Kvantovuyu Statisticheskuyu Mekhaniku* (Moscow: Nauka, 1984)
66. Ketterle W, van Druten N J *Phys. Rev. A* **54** 656 (1996)
67. Reatto L, Chester G V *Phys. Rev.* **155** 88 (1967)
68. Sonin É B *Sov. Phys. JETP* **32** 773 (1971); *Zh. Eksp. Teor. Fiz.* **59** 1416 (1970)
69. Berezinskii V L *Sov. Phys. JETP* **34** 610 (1972); *Zh. Eksp. Teor. Fiz.* **61** 1144 (1971)
70. Popov V N *Theor. Math. Phys.* **11** 565 (1972); *Teor. Matem. Fiz.* **11** 354 (1972)
71. Lozovik Yu E, Yudson V I *JETP Lett.* **22** 274 (1975); *Pis'ma Zh. Eksp. Teor. Fiz.* **22** 556 (1975)
72. Lozovik Yu E, Yudson V I *Physica A* **93** 493 (1978)
73. Lieb E H, Liniger W *Phys. Rev.* **130** 1605 (1963)
74. Lieb E H *Phys. Rev.* **130** 1616 (1963)
75. Ovchinnikov A A *JETP Lett.* **57** 477 (1993); *Pis'ma Zh. Eksp. Teor. Fiz.* **57** 458 (1993)
76. Snoke D et al. *Nature* **418** 754 (2002)
77. Stern M, Umansky V, Bar-Joseph I *Science* **343** 55 (2014)
78. Gammon D et al. *Phys. Rev. Lett.* **76** 3005 (1996)
79. Semina M A, Sergeev R A, Suris R A *Semiconductors* **40** 1338 (2006); *Fiz. Tekh. Poluprovodn.* **40** 1373 (2006)
80. Evers F, Mirlin A D *Rev. Mod. Phys.* **80** 1355 (2008)
81. Lifshitz I M *Sov. Phys. JETP* **26** 462 (1968); *Zh. Eksp. Teor. Fiz.* **53** 743 (1967)
82. Lifshits I M, Gredeskul S A, Pastur L A *Introduction to the Theory of Disordered Systems* (New York: Wiley, 1988); Translated from Russian: *Vvedenie v Teoriyu Neuporyadochennykh Sistem* (Moscow: Nauka, 1982)
83. Griffin A, Snoke D W, Stringari S *Bose – Einstein Condensation* (Cambridge: Cambridge Univ. Press, 1995)
84. Pitaevskii L, Stringari S *Bose – Einstein Condensation* (Intern. Series of Monographs on Physics, Vol. 116) (Oxford: Clarendon Press, 2003)
85. Bagnato V, Kleppner D *Phys. Rev. A* **44** 7439 (1991)
86. Thomas D G, Hopfield J J, Augustyniak W M *Phys. Rev.* **140** A202 (1965)
87. Golub L E, Ivchenko E L, Kiselev A A *J. Opt. Soc. Am. B* **13** 1199 (1996)
88. Kiselev A A *Semiconductors* **32** 504 (1998); *Fiz. Tekh. Poluprovodn.* **32** 564 (1998)
89. Tarasenko S A et al. *Semicond. Sci. Technol.* **16** 486 (2001)
90. Shklovskii B I, Efros A L *Electronic Properties of Doped Semiconductors* (Springer Series in Solid-State Sciences, Vol. 45) (Berlin: Springer-Verlag, 1984); Translated from Russian: *Elektronnye Svoistva Legirovannykh Poluprovodnikov* (Moscow: Nauka, 1979)
91. Sugakov V I *J. Phys. Condens. Matter* **31** 475301 (2019)
92. Landau L D, Lifshitz E M *Quantum Mechanics*: *Non-Relativistic Theory* (Oxford: Pergamon Press, 1977); Translated from Russian: *Kvantovaya Mekhanika*: *Nerelyativistskaya Teoriya* (Moscow: Nauka, 1974)
93. Ciuti C et al. *Phys. Rev. B* **58** 7926 (1998)
94. Baas A et al. *Phys. Rev. Lett.* **100** 170401 (2008)
95. Wouters M *Phys. Rev. B* **77** 121302(R) (2008)
96. Ohadi H et al. *Phys. Rev. B* **97** 195109 (2018)
97. Malpuech G et al. *Phys. Rev. Lett.* **98** 206402 (2007)
98. Kovalev V M, Chaplik A V *JETP Lett.* **92** 185 (2010); *Pis'ma Zh. Eksp. Teor. Fiz.* **92** 208 (2010)
99. Baranovski S (Ed.) *Charge Transport in Disordered Solids with Applications in Electronics* (Chichester: Wiley, 2006)
100. Pethick C J, Smith H *Bose–Einstein Condensation in Dilute Gases* (Cambridge: Cambridge Univ. Press, 2002)
101. Basko D M, Aleiner I L, Altshuler B L *Ann. Physics* **321** 1126 (2006)
102. Lozovik Yu E, Berman O L, Ruvinskii A M *JETP Lett.* **69** 616 (1999); *Pis'ma Zh. Eksp. Teor. Fiz.* **69** 573 (1999)
103. Astrakhartchik G "Properties of a Bose gas in the presence of disorder", Ph.D. Thesis (Trento: Univ. Degli Studi di Trento, 2000 – 2001)
104. Berman O L et al. *Phys. Rev. B* **70** 235310 (2004)
105. Gaul C, Müller C A *Phys. Rev. A* **83** 063629 (2011)
106. Müller C A, Gaul C *New J. Phys.* **14** 075025 (2012)
107. Glazov M M et al. *Phys. Rev. B* **88** 041309(R) (2013)
108. Laussy F P et al. *Phys. Rev. Lett.* **93** 016402 (2004)
109. Laussy F P, in *Exciton Polaritons in Microcavities* (Springer Series in Solid-State Sciences, Vol. 172, Eds V Timofeev, D Sanvitto) (Berlin: Springer-Verlag, 2012) p. 1
110. Henry C H, Kazarinov R F *Rev. Mod. Phys.* **68** 801 (1996)
111. Wouters M, Carusotto I *Phys. Rev. Lett.* **99** 140402 (2007)
112. Carusotto I, Ciuti C *Rev. Mod. Phys.* **85** 299 (2013)
113. Keeling J, Berloff N G *Phys. Rev. Lett.* **100** 250401 (2008)
114. Keeling J, Berloff N G *Contemp. Phys.* **52** 131 (2011)
115. Gippius N A, Tikhodeev S G *J. Phys. Condens. Matter* **16** S3653 (2004)
116. Gippius N A et al *Phys. Usp.* **48** 306 (2005); *Usp. Fiz. Nauk* **175** 327 (2005)
117. Elistratov A A, Lozovik Yu E *Phys. Rev. B* **97** 014525 (2018)
118. Porras D, Tejedor C *Phys. Rev. B* **67** 161310(R) (2003)
119. Schawlow A L, Townes C H *Phys. Rev.* **112** 1940 (1958)
120. Lax M *Phys. Rev.* **160** 290 (1967)
121. Hanai R et al. *Phys. Rev. Lett.* **122** 185301 (2019)
122. Gavrilov S S *Phys. Usp.* **63** 123 (2020); *Usp. Fiz. Nauk* **190** 137 (2020)
123. Khalatnikov I M *Teoriya Sverkhtekuchesti* (The Theory of Superfluidity) (Moscow: Nauka, 1971)
124. Brusov P N, Popov V N *Sverkhtekuchest' i Kollektivnye Svoistva Kvantovykh Zhidkostei* (Superfluidity and Collective Properties of Quantum Fluids) (Moscow: Nauka, 1988)
125. Roumpos G et al. *Proc. Natl. Acad. Sci. USA* **109** 6467 (2012)
126. Mouchliadis L, Ivanov A L *Phys. Rev. B* **78** 033306 (2008)
127. High A A et al. *Nature* **483** 584 (2012)
128. Yang S et al. *Phys. Rev. Lett.* **97** 187402 (2006)
129. Deng H et al. *Phys. Rev. Lett.* **99** 126403 (2007)
130. Nardin G et al. *Phys. Rev. Lett.* **103** 256402 (2009)
131. Kasprzak J et al. *Phys. Rev. Lett.* **101** 146404 (2008)
132. Lagoudakis K G et al. *Nat. Phys.* **4** 706 (2008)
133. Amo A et al. *Nature* **457** 291 (2009)
134. Byrnes T, Kim N Y, Yamamoto Y *Nat. Phys.* **10** 803 (2014)
135. Amo A et al. *Science* **332** 1167 (2011)
136. Sich M et al. *Nat. Photon.* **6** 50 (2012)
137. Cilibrizzi P et al. *Phys. Rev. Lett.* **113** 103901 (2014)
138. Eisenstein J P, MacDonald A H *Nature* **432** 691 (2004)
139. Eisenstein J P, Pfeiffer L N, West K W *Phys. Rev. Lett.* **123** 066802 (2019)
140. Kulik L V et al. *Nat. Commun.* **7** 13499 (2016)
141. Kulik L V et al. *Phys. Usp.* **62** 865 (2019); *Usp. Fiz. Nauk* **189** 925 (2019)
142. Lampert M A *Phys. Rev. Lett.* **1** 450 (1958)
143. de-Leon S B-T, Laikhtman B *Phys. Rev. B* **63** 125306 (2001)
144. Combescot M, Betbeder-Matibet O, Dubin F *Phys. Rep.* **463** 215 (2008)
145. Schindler C, Zimmermann R *Phys. Rev. B* **78** 045313 (2008)
146. Walther V et al. *Phys. Rev. B* **98** 165201 (2018)
147. Huang K *Phys. Rev.* **119** 1129 (1960)

148. Iordanskii S V *Sov. Phys. JETP* **20** 112 (1965); *Zh. Eksp. Teor. Fiz.* **47** 167 (1964)
149. Lee T D, Huang K, Yang C N *Phys. Rev.* **106** 1135 (1957)
150. Schick M *Phys. Rev. A* **3** 1067 (1971)
151. Hines D, Frankel N E, Mitchell D J *Phys. Lett. A* **68** 12 (1978)
152. Fisher D S, Hohenberg P C *Phys. Rev. B* **37** 4936 (1988)
153. Lieb E H, Yngvason J *J. Stat. Phys.* **103** 509 (2001)
154. Mora C, Castin Y *Phys. Rev. Lett.* **102** 180404 (2009)
155. Beane S R *Phys. Rev. A* **82** 063610 (2010)
156. Fournais S et al. *J. Math. Phys.* **60** 071903 (2019)
157. Khrapak S A, Kryuchkov N P, Yurchenko S O *Phys. Rev. E* **97** 022616 (2018)
158. Couëdel L et al. *Phys. Usp.* **62** 1000 (2019); *Usp. Fiz. Nauk* **189** 1070 (2019)
159. Misra S et al. *Phys. Rev. Lett.* **120** 047402 (2018)
160. Pokrovskii Ya E, Svistunova K I *JETP Lett.* **9** 261 (1969); *Pis'ma Zh. Eksp. Teor. Fiz.* **9** 435 (1969)
161. Sibel'din N N *J. Exp. Theor. Phys.* **122** 587 (2016); *Zh. Eksp. Teor. Fiz.* **149** 678 (2016)
162. Sager L M, Safaei S, Mazziotti D A *Phys. Rev. B* **101** 081107(R) (2020)
163. Navon N et al. *Science* **328** 729 (2010)
164. Kagan M Yu, Turlapov A V *Phys. Usp.* **62** 215 (2019); *Usp. Fiz. Nauk* **189** 225 (2019)
165. Wang G et al. *Rev. Mod. Phys.* **90** 021001 (2018)
166. Tartakovskii A *Nat. Rev. Phys.* **2** 8 (2020)
167. Waldherr M et al. *Nat. Commun.* **9** 3286 (2018)
168. Arp T B et al. *Nat. Photon.* **13** 245 (2019)